Published in final edited form as:
J Mol Biol. 2011 February 18; 406(2): 257–274. doi:10.1016/j.jmb.2010.11.042.

The human mitochondrial tRNA^{Met}: Structure/function relationship of a unique modification in the decoding of unconventional codons

Yann Bilbille[1,†], **Estella M. Gustilo**[1,†], **Kimberly A. Harris**[1], **Christie N. Jones**[2], **Hrvoje Lusic**[3], **Robert J. Kaiser**[4], **Michael O. Delaney**[4], **Linda L. Spremulli**[2], **Alexander Deiters**[3], and **Paul F. Agris**[1,*]

[1]Department of Molecular and Structural Biochemistry, North Carolina State University, Raleigh, NC 27695, USA

[2]Department of Chemistry, University of North Carolina, Chapel Hill, NC 27599, USA

[3]Department of Chemistry, North Carolina State University, Raleigh, NC 27695, USA

[4]Thermo Fisher Scientific, 2650 Crescent Drive #100, Lafayette, CO 80026, USA

Abstract

Human mitochondrial mRNAs utilize the universal AUG and the unconventional isoleucine AUA codons for methionine. In contrast to translation in the cytoplasm, human mitochondria use one tRNA, hmtRNA$^{Met}_{CAU}$, to read AUG and AUA codons at both the peptidyl- (P-), and aminoacyl- (A-) sites of the ribosome. The hmtRNA$^{Met}_{CAU}$ has a unique post-transcriptional modification, 5-formylcytidine, at the wobble position 34 (f^5C_{34}), and a cytidine substituting for the invariant uridine at position 33 of the canonical "U-turn" in tRNAs. The structure of the tRNA's anticodon stem and loop domain (hmtASL$^{Met}_{CAU}$), determined by NMR restrained molecular modeling, revealed how the f^5C_{34} modification facilitates the decoding of AUA at the P- and A-sites. The f^5C_{34} defined a reduced conformational space for the nucleoside, in what appears to have restricted the conformational dynamics of the anticodon bases of the modified hmtASL$^{Met}_{CAU}$. The hmtASL$^{Met}_{CAU}$ exhibited a "C-turn" conformation that has some characteristics of the U-turn motif. Codon binding studies with both *E. coli* and bovine mitochondrial ribosomes revealed that the f^5C_{34} facilitates AUA binding in the A-site and suggested that the modification favorably alters the ASL's binding kinetics. Mitochondrial translation by many organisms including humans sometimes initiates with the universal isoleucine codons AUU and AUC. The f^5C_{34} enabled P-site codon binding to these normally isoleucine codons. Thus, the physicochemical properties of this

[*]Corresponding authors present address: The RNA Institute, University at Albany-SUNY, 1400 Washington Ave., Albany, NY 12222, USA; Tel: 518-437-4448; FAX: 518-437-4456; PAgris@albany.edu.
[†]Y.B. and E.M.G. have contributed equally to this manuscript. The manuscript is in partial fulfillment of the Ph.D. by E.M.G.

Present Addresses:
Estella M. Gustilo: Department of Molecular & Experimental Medicine, The Scripps Research Institute, 10550 N. Torrey Pines Rd. MEM 220, La Jolla, CA 92037 estellag@scripps.edu
Kimberly A. Harris: The RNA Institute, Biological Sciences, University at Albany-SUNY, 1400 Washington Ave., Albany, NY 12222, USA: kh499288@albany.edu
Christie N. Jones: UT Health Science Center San Antonio, TX 78229-3900; jonesc7@uthscsa.edu
Yann Bilbille: 3 Route Notre Dame des Puits Godeneval, 28350 Dampierre sur Avre, France

Accession numbers: PDB code:2KRZ (hmtASL$^{Met}_{CAU}$-Ψ_{27}); 2KRY (hmtASL$^{Met}_{CAU}$-Ψ_{27};f^5C); BMRB entry: 16655 (hmtASL$^{Met}_{CAU}$-Ψ_{27}), 16654 (hmtASL$^{Met}_{CAU}$-Ψ_{27};f^5C)

one modification, f^5C_{34}, expand codon recognition from the traditional AUG to the non-traditional, synonymous codons AUU and AUC as well as AUA, in the reassignment of universal codons in the mitochondria.

Keywords

5-formylcytidine; NMR structure; mitochondrial translation; codon expansion; near cognate decoding

Introduction

Mitochondria are membrane-bound organelles with their own genetic information. Through oxidative phosphorylation, the organelle generates the majority of the eukaryotic cell's energy resource, ATP. Most of the approximately 2000 proteins that compose the mitochondrion are encoded by nuclear DNA and are imported. However, the mitochondrial genome encodes thirteen critical components of the electron transfer chain and the ATP synthase. These proteins are the only products of the organelle's protein synthesizing machinery. Other components required for translation, including the ribosomal proteins and the auxiliary initiation, elongation and termination factors, are the products of nuclear genes. The mammalian mitochondrial DNA also encodes 22 tRNAs (mtRNA), one for each of 18 amino acids and two each for serine and leucine.[1] Cytoplasmic tRNAs are not imported into the mammalian mitochondria,[2] perhaps with the one exception of cytoplasmic glutamine tRNA imported into the isolated mitochondria of cells from individuals with myoclonic epilepsy with ragged-red fiber (MERRF).[3]

This minimal set of 22 mtRNAs must respond to all of the amino acid codons. In order to facilitate the reading of the amino acid codes in mammalian mitochondria, an unmodified uridine in the “wobble” position 34 of the mtRNA recognizes all four nucleotides at the third position of the synonymous codons, a guanine in position 34 recognizes only pyrimidines, and a modified uridine discriminates between purines and pyrimidines.[4] Thus, there are some exceptions to the reading of the universal genetic code. Sequence analysis of mitochondrial genomes from various organisms has revealed that there are many codon reassignments, a unique feature of the non-plant mitochondrial translational systems.[4,5] For example, in mammalian mitochondria the universal stop codon UGA codes for tryptophan, and the two universal arginine codons AGA and AGG either terminate translation, or promote frameshifting in the human mitochondrial ribosome.[6] Of particular interest is the universal isoleucine codon AUA that is used to specify methionine for initiation and elongation of translation.[1,7-10]

In the cytoplasm, two $tRNA^{Met}_{CAU}$ decode the single methionine codon AUG.[1] One is an initiator tRNA ($tRNA_i^{Met}_{CAU}$ for eukaryotes and $tRNA_f^{Met}_{CAU}$ for prokaryotes) that decodes AUG in the ribosome's peptidyl- or P-site at the initiation of translation. The other $tRNA^{Met}_{CAU}$ is responsible for recognizing the AUG codons internal to the mRNA ($tRNA_m^{Met}_{CAU}$). In contrast, the single mitochondrial $tRNA^{Met}_{CAU}$ plays a unique role since it supports both the initiation and elongation of protein synthesis by responding to the universal methionine codon AUG in the A- and P-sites.[10] The $tRNA^{Met}_{CAU}$ anticodon is the Watson-Crick complement for the methionine codon AUG. This single $mtRNA^{Met}_{CAU}$ also reads the codon AUA which is present in mitochondrial mRNAs as 20% of the initiator codons, and 80% of internal methionine codons. Francis Crick's Wobble Hypothesis explained how a tRNA would be able to read more than one codon, but also predicted an unfavorable pairing of the anticodon CAU to the codon AUA due to the C●A mismatch at the wobble position.[11] Since the AUA codon occurs much more frequently than the AUG

codon in mammalian mitochondrial genomes,[1] it has been assumed that some special mechanism must exist in the mitochondrial translation system to allow the AUA codon to be translated as methionine.

The unique post-transcriptional modification at the human mtRNA$^{Met}_{CAU}$ (hmtRNA$^{Met}_{CAU}$) wobble position 34, 5-formylcytidine (f^{5}C$_{34}$) (Fig. 1c),[12,13] may play a crucial role in the recognition of both methionine codons, the non-universal AUA and the universal AUG.[14,15] The hmtRNA$^{Met}_{CAU}$ shares an important similarity to elongator tRNA$^{Met}_{CAU}$ in that both have a wobble position-34 modification; in *Escherichia coli* the modification is N^4-acetylcytidine, while in humans it is 2′-*O*-methylcytidine.[16] The bacterial and eukaryotic cytoplasmic initiator tRNA$^{Met}_{CAU}$ are unmodified at the wobble position. The f^{5}C modification has been found in the mitochondrial tRNA$^{Met}_{CAU}$ of humans, bovines, and rodents and is considered universal in mammalian mtRNA$^{Met}_{CAU}$.[10,13,17] The modification also is found in the mtRNA$^{Met}_{CAU}$ of nematodes, squids, frogs, chickens, and fruit flies.[4,13,18,19] Human mtRNA$^{Met}_{CAU}$ is a hybrid of the mammalian cytoplasmic initiator and elongator tRNA$^{Met}_{CAU}$ species. The hmtRNA$^{Met}_{CAU}$ has the three consecutive G-C pairs at the bottom of the anticodon stem characteristic of initiator tRNAs (Fig. 1). However, this tRNA has a number of unusual features. The dihydrouridine (D)-loop of the human mitochondrial tRNA$^{Met}_{CAU}$ is smaller than that of the canonical cytoplasmic tRNAs and lacks the G residues at 18 and 19 that normally facilitate interactions with the T-loop. The minor loop is small and does not contain the common residue G47. The T-stem has two adjacent pyrimidine:pyrimidine pairs (U-U and U-Ψ). The T-loop lacks the TΨC sequence and contains only 6 nucleotides instead of the normal seven. There is also a mismatch in the acceptor stem.

Our studies focus on the folding, structure and codon binding properties of the hmtRNA$^{Met}_{CAU}$,[15,20,21] in particular that of tRNA's anticodon stem and loop domain, hmtASL$^{Met}_{CAU}$.[15] The heptadecamer hmtASL$^{Met}_{CAU}$ has a five base-paired stem consisting of the three contiguous G●C/C●G base pairs (residues 29–31/39–41) that are proximal to the loop and contribute thermodynamic stability to the RNA through stacking (Fig. 1) - a hallmark of initiator tRNA^{Met} that increases its affinity for the P-site.[22] As with the mammalian initiator tRNA^{Met}, the hmtASL$^{Met}_{CAU}$ has a cytidine at position-33. The 33rd residue of tRNAs is usually occupied by the invariant U$_{33}$, responsible for the “U-turn” in the backbone that presents the anticodon for codon binding. Other than in the hmtASL$^{Met}_{CAU}$, C$_{33}$ has been found only in the cytoplasmic initiator tRNA$^{Met}_{CAU}$ of insects, plants, and vertebrates.[16] In the yeast initiator tRNA$_i^{Met}_{CAU}$, the loop is closed by a non-canonical C$_{32}$●A$_{38}$ base-pair, whereas in the hmtRNA$^{Met}_{CAU}$ the loop has only the potential of a non-canonical C$_{32}$●C$_{38}$ base pair. Position 37, 3′-adjacent to the anticodons of many of the cytoplasmic tRNA$_{i,f}^{Met}_{CAU}$ and tRNA$_m^{Met}_{CAU}$, have the t^{6}A modification, or a variant,[16] whereas the hmtRNA$^{Met}_{CAU}$ has no modification at position 37. Previously, we had reported the procedures for chemical synthesis of the f^{5}C mononucleoside and for its successful, site-selected incorporation into the hmtASL$^{Met}_{CAU}$.[15] In the present paper, we use this chemistry to explore in detail the impact of the modification on the structure and dynamics of the ASL, and the biological ramifications of the formyl modification in the hmtASL$^{Met}_{CAU}$ recognition of non-cognate codons. In our initial report the 5-formyl group appeared to be significant to the binding of the unconventional methionine codon AUA.[15] The introduction of the f^{5}C modification lowered the melting temperature and ellipticity, suggesting that this modification can enhance the dynamic of the loop[15]. Thus, the unique modification such as the f^{5}C can represent a powerful tool in the stabilization of the codon-anticodon interaction. Nevertheless, how the mtRNA^{Met} interacts with the mRNA into the ribosome still remained unclear. Further, ribosome binding experiments using native tRNA$^{Met}_{CAU}$ having the normal modifications and an unmodified transcript of tRNA$^{Met}_{CAU}$ indicate that f^{5}C is important for decoding in the A-site of the bovine mitochondrial

ribosome.[14] We have sought to understand the role of the 5-formyl group in the efficiency of binding of the hmtRNA$^{Met}_{CAU}$ to the mitochondrial codons AUA or AUG at both the ribosomal P- or A-sites. Here, we report the first high resolution three dimensional structures of the modified and unmodified human mitochondrial anticodon domain of tRNA$^{Met}_{CAU}$. The conformational dynamic of the hmtASL$^{Met}_{CAU}$ appears to be influenced by the f^5C_{34} modification in the direction of enhanced order in the anticodon loop. In addition, we demonstrate that the wobble position f^5C_{34} of hmtRNA$^{Met}_{CAU}$ is particularly important to the binding of the hmtASL$^{Met}_{CAU}$ to AUA at the A-site. Interestingly, some organisms use the isoleucine codons AUU and AUC in initiation of translation at the P-site.[9,18,23-25] The structure and dynamics of the anticodon may be critical to recognition of the unconventional AUA codon at the P- and A-sites of the ribosome, and in expanding its P-site recognition further to AUU and AUC.

Results

In order to determine the effect of f^5C_{34} on codon recognition and its physicochemical contribution to the conformation and dynamics of the hmtASL$^{Met}_{CAU}$, we have solved the solution structures of the hmtASL$^{Met}_{CAU}$-Ψ_{27} and the hmtASL$^{Met}_{CAU}$-Ψ_{27};f^5C_{34} by NMR and restrained molecular modeling. In addition, we have analyzed the codon binding of the ASLs and the full length tRNA with *E. coli* and bovine mitochondrial ribosomes. The heptadecamer hmtASL$^{Met}_{CAU}$ constructs were chemically synthesized with pseudouridine at the 5′-terminal position 27 (Ψ_{27}), and with or without f^5C_{34}. The ASLs are designated hmtASL$^{Met}_{CAU}$-Ψ_{27};f^5C_{34} and hmtASL$^{Met}_{CAU}$-Ψ_{27}, respectively (Fig. 1).

Contribution of f^5C_{34} to the structure of the hmtRNA$^{Met}_{CAU}$ anticodon: NMR resonance assignments

The structural contributions of f^5C_{34} to the hmtASL$^{Met}_{CAU}$ were determined by NMR-restrained molecular modeling. The non-exchangeable resonances were assigned using well established techniques.[26] The 1D spectrum recorded exhibited three sharp peaks in the imino region which were assigned to G_{29}, G_{30} and G_{31} imino proton resonances, involved in canonical G●C base pairing (Fig. 2a). One other resonance, broader than the previous ones, at 11.0 ppm was assigned to Ψ_{27}H3 (Fig. 2a) and two NOE connectivities were observed between Ψ_{27}H3 and the amino group of A_{43}. The NMR data clearly demonstrated that the stem residues (C_{28} – G_{31} and C_{39} – G_{42}) adopt a classical A-form RNA structure. The sequential pathway (aromatic to H1′ of the 3′ residue) could be followed using the 400ms NOESY spectrum from Ψ_{27} to C_{33} and from A_{37} to G_{43} (Fig. 3). A break appeared between C_{33} and f^5C_{34}/C_{34}, however, a weak sequential NOE was observed at 400 ms between f^5C_{34}/C_{34} H1′ and A_{35}H8. The two ASLs exhibited non-sequential NOEs between the A_{35}H8 and C_{33}H1′/H2′ protons. No NOE connectivity was observed between A_{35}H8 and U_{36}H1′, nor between U_{36}H6 and A_{37}H1′, even with a long mixing time (400ms). On the 5′ side of the loop, C_{32} was stacked with G_{31} and C_{33}, as shown by the inter-aromatic NOEs between the bases (C_{32}H5/G_{31}H8, C_{32}H6/G_{31}H8, C_{32}H6/C_{33}H6 and C_{32}H6/C_{33}H5). Moreover, the chemical shifts of C_{38} and the C_{32}H5/H6 protons were characteristic of protons experiencing a 5′ purine ring current,[26] confirming the stacking of G_{31}/C_{32}, and of A_{37}/C_{38}. The A_{37}H2 resonance was identified based on the natural abundance ^1H-^{13}C HSQC spectrum and a strong NOE connectivity was observed between the A_{37}H2 and C_{38}H1′. Non-sequential NOEs were observed between A_{35}H2 and A_{37}H1′, as well as between A_{35}H2 and A_{37}H8 (Fig. 3). The chemical shifts of U_{36}H5 and H6 were not in agreement with the chemical shift of a uridine experiencing a purine ring current, and thus were not supportive of the stacking of A_{35} and U_{36}. Moreover, weak NOEs were observed between U_{36}H6 and the A_{35}H3′/H2′ protons, as well as very weak NOEs between U_{36}H5 and A_{35}H3′, and H2′. Weak inter-aromatic NOEs were observed between A_{37}H8 and

U_{36}H6 and between U_{36}H6 and A_{35}H8. Nevertheless, the intensities of these NOE connectivities were less than the NOE between A_{35}H2 and A_{37}H1′ (Fig. 3). A considerable number of inter-residue NOEs were observed for the hmtASL$^{Met}_{CAU}$-Ψ_{27};f^5C_{34} and the hmtASL$^{Met}_{CAU}$-Ψ_{27}. The inter-nucleoside NOEs of the anticodon loop residues (C_{32}-C_{38}) were particularly important to establishing the contribution of the f^5C_{34}. A significant number of these were attributed to the modified nucleoside, and to C_{33} and A_{35} (Fig. 4).

Sugar conformations and backbone geometry

All of the loop residues, with one exception, exhibited small to very small $^3J_{H1'-H2'}$ coupling constants corresponding to the *C3′-endo* sugar pucker conformation. The COSY spectra indicated that U_{36} adopted a *C2′-endo* sugar pucker conformation. The ^{31}P phosphorous spectra of both ASLs showed that all the resonances are grouped together within ± 0.5 ppm except for three resonances belonging to the residues f^5C_{34}/C_{34}, U_{36} and A_{37} (Fig. 2b,c). The phosphorous resonance of C_{34} was downfield by 0.9 ppm from the ^{31}P main cluster, whereas the f^5C_{34} ^{31}P resonance was downfield by 1.1ppm (Fig. 2b,c). The ^{31}P resonance of A_{37} was slightly downfield (~0.3 ppm), whereas that of U_{36} was upfield (~0.3 ppm) from the main cluster of peaks. All of the other resonances remained in the main cluster, indicating that the α and ζ angles were typical of an A-form RNA conformation (Fig. 2b,c).

Structures of the hmtASL$^{Met}_{CAU}$-Ψ_{27};f^5C_{34} and the hmtASL$^{Met}_{CAU}$-Ψ_{27}

The structures of the hmtASL$^{Met}_{CAU}$-Ψ_{27};f^5C_{34} and hmtASL$^{Met}_{CAU}$-Ψ_{27} were derived from the NMR data using a simulated annealing protocol.[26] Ten of the lowest energy structures for the hmtASL$^{Met}_{CAU}$ Ψ_{27};f^5C_{34} and for the hmtASL$^{Met}_{CAU}$-Ψ_{27} were superimposed (Fig. 5). The stems of both ASLs adopt a classical A-form RNA conformation. The ten lowest energy structures for the hmtASL$^{Met}_{CAU}$-Ψ_{27};f^5C_{34} and for the hmtASL$^{Met}_{CAU}$-Ψ_{27} had overall heavy atom RMSDs relative to the mean structure of 1.71 ± 0.58 Å and 1.51 ± 0.46 Å, respectively (Table 1). The C_{32}●C_{38}, C1′ – C1′ distance was on average 10.19 ± 0.54 Å and 10.39 ± 0.35 Å for the hmtASL$^{Met}_{CAU}$-Ψ_{27};f^5C_{34} and for the hmtASL$^{Met}_{CAU}$-Ψ_{27}, respectively. These values are comparable to the classical A-RNA C1′-C1′ distance (~10.6 Å). The heavy atom RMSD value observed for the loop residues (C_{32} to C_{38}) relative to the mean structure were 0.38 ± 0.20 Å and 0.51 ± 0.17 Å, respectively.

The two loops (C_{32} to C_{38}) exhibited the same overall conformation (Fig. 6). The stem was continued from the canonical base pair G_{31}●C_{39} at the bottom of the stem through the non-canonical C_{32}●C_{38} mismatch pair (Fig. 6c). Taken together with the stacking of G_{31}/C_{32} and C_{39}/C_{38}, the C_{32}●C_{38} non-canonical base pair extended the stem. In the loop, the position of C_{32} was stabilized by a hydrogen bond between the C_{32}O2 and the C_{38}N4 with acceptor-donor distances of 2.98 ± 0.15 Å and 3.30 ± 0.20 Å for the hmtASL$^{Met}_{CAU}$-Ψ_{27};f^5C_{34} and for the hmtASL$^{Met}_{CAU}$-Ψ_{27}, respectively. Moreover, the structures were stabilized by a probable hydrogen bond between C_{32}N4 and A_{37}O2P with acceptor donor distances of 3.12 ± 0.47 Å and 3.49 ± 0.48 Å for the hmtASL$^{Met}_{CAU}$-Ψ_{27};f^5C_{34} and for the hmtASL$^{Met}_{CAU}$-Ψ_{27}, respectively.

In both ASLs, the unusual C_{33} residue was stacked with C_{32}. An abrupt turn in the backbone was observed between the residues C_{33} and f^5C_{34}/C_{34} (Fig. 6a and b) The turn was characterized by a trans α dihedral angle (173 ± 20° for hmtASL$^{Met}_{CAU}$-Ψ_{27};f^5C and -160.5 ± 8.6° for hmtASL$^{Met}_{CAU}$-Ψ_{27}). The f^5C_{35}/C_{34} and A_{35} residues were stacked nicely, consistent with the observation of n/n+2 NOEs between the two residues in the NMR spectra. Both nucleosides adopted the *C3′-endo* sugar conformation. The average distance between the C_{33}2′OH and the A_{35}N7 was 2.88 ± 0.08 Å and 2.90 ± 0.07 Å for the

hmtASL$^{Met}_{CAU}$-Ψ$_{27}$;f^{5}C$_{34}$ and for the hmtASL$^{Met}_{CAU}$-Ψ$_{27}$, respectively, allowing the formation of a direct hydrogen bond. In both structures, the U$_{36}$ adopted the *C2′-endo* sugar pucker conformation (δ dihedral angles of 137.9 ± 4.6° for hmtASL$^{Met}_{CAU}$-Ψ$_{27}$;f^{5}C and 143.1 ± 1.6° for hmtASL$^{Met}_{CAU}$-Ψ$_{27}$), which is consistent with the NMR data. Thus, the base resides outside the loop and in direct contact with the solvent. The intra-residue NOEs of f^{5}C$_{34}$ include those between the formyl proton and H6 and H1′. These fix the position of the formyl proton relative to the nucleoside conformation. In addition, there are weak NOEs between the formyl proton and A$_{35}$H8 and the formyl proton and C$_{33}$H3′. Importantly, the conformational space occupied by the f^{5}C$_{34}$ in the ten structures of hmtASL$^{Met}_{CAU}$-Ψ$_{27}$;f^{5}C$_{34}$ was considerably less than that occupied by C$_{34}$ within the ten structures of hmtASL$^{Met}_{CAU}$-Ψ$_{27}$. The limited space that confined the motional dynamics of the modification may be indicative of the modification's contributions to the reading of unconventional codons.

The anticodon wobble position modification, 5-formylcytidine, enhances AUA A-site codon recognition by the hmtASL$^{Met}_{CAU}$-Ψ$_{27}$;f^{5}C$_{34}$

Mitochondrial tRNA^{Met} must recognize both AUG and AUA in the P-site for initiation and in the A-site during polypeptide chain elongation. To study the effect of the f^{5}C$_{34}$ residue on the codon binding characteristics of the human mitochondrial tRNA^{Met}, we determined the equilibrium binding properties of the hmtASL$^{Met}_{CAU}$-Ψ$_{27}$, with and without the f^{5}C$_{34}$ to the AUG and AUA codons at the P- and A-sites by titrating mRNA-programmed, *E. coli* 70S ribosomes with increasing amounts of the hmtASL$^{Met}_{CAU}$ (Fig. 7; Table 2). As would be expected,[27] the two ASLs bound the P-site codons to a degree (3-4 pmoles bound) exceeding by several fold their binding of the A-site codons (0.5-1.0 pmoles). The 5-formyl modification did not affect the equilibrium binding of hmtASL$^{Met}_{CAU}$-Ψ$_{27}$;f^{5}C$_{34}$ to AUG at the P- site (Table 2). Neither the dissociation constant, nor the extent of binding to AUA, at the P-site appear to be affected greatly by the f^{5}C$_{34}$ modification (Table 2; Fig. 7a). In binding AUA at the P-site, the hmtASL$^{Met}_{CAU}$-Ψ$_{27}$;f^{5}C$_{34}$ and the hmtASL$^{Met}_{CAU}$-Ψ$_{27}$ exhibited steady-state dissociation constants within experimental error of each other, 7.9 ± 5.5 μM and 11.0 ± 4.7 μM, respectively. Binding to AUA in the P-site was weak resulting in larger errors in the determination of the K_ds. The most striking observation in this data is that the extent of either hmtASL$^{Met}_{CAU}$-Ψ$_{27}$;f^{5}C$_{34}$ or hmtASL$^{Met}_{CAU}$-Ψ$_{27}$ binding at the P-site was substantially lower than observed with the AUG codon. The differences in saturation level between binding to AUA and binding to AUG probably arises from differences in kinetics. First, there appears to be an intrinsically lower ability of the hmtASL$^{Met}_{CAU}$ to capture the formed complex when AUA is present. This is most likely a consequence of the difficulty of forming the f^{5}C$_{34}$-A base pair and the weakness of this pairing. We suspect that on the *E. coli* ribosome two pathways to codon binding occur, as has been reviewed previously.[28] In one, the ASL binds before the mRNA, but leaves rapidly due to unstable interactions. In the other, the mRNA binds first via the Shine-Delgarno sequence, but also dissociates rapidly in the absence of codon:anticodon interactions. Thus, stable binding of the ASL is only observed when both hmtASL$^{Met}_{CAU}$ and mRNA are present at the same time leading to codon:anticodon interactions. With AUA, the kinetics of the codon:anticodon interaction and/or the stability of the interaction is weaker than that with AUG and the complex cannot form to the same extent. Therefore, the major difference in saturation is that attributed to differences in codon:anticodon interactions. This observation suggests that the use of AUA as the initiation codon may reduce the efficiency of initiation complex formation for specific mRNAs in mammalian mitochondria.

The f^{5}C$_{34}$-modified hmtASL$^{Met}_{CAU}$-Ψ$_{27}$ bound AUG in the A-site with a higher affinity than that of the hmtASL$^{Met}_{CAU}$-Ψ$_{27}$ as indicated by the lower dissociation constant (Table 2; Fig. 7b). At the A-site, the hmtASL$^{Met}_{CAU}$-Ψ$_{27}$;f^{5}C$_{34}$ bound AUA with a K_d of 1.6 ± 0.4

μM (Fig. 7b; Table 2). However, the hmtASL$^{Met}_{CAU}$-Ψ$_{27}$ exhibited a a higher K_d of 4.5 ± 2.1 μM. Thus, there appears to be a modification-dependent difference in the hmtASL binding of AUA at the A-site. Again, the largest difference observed in the AUG versus AUA-dependent binding at the A-site is reflected in a lower extent of binding suggesting that the off-rate for codon-anticodon interactions could be more rapid with the AUA codon.

Kinetics of the f^{5}C$_{34}$-modified and unmodified hmtASL$^{Met}_{CAU}$-Ψ$_{27}$ binding AUG and AUA at the P- and A-site

The unmodified CAU anticodon of tRNA^{Met} is a canonical match for the codon AUG. Therefore, we did not expect the 5-formyl modification of hmtASL$^{Met}_{CAU}$-Ψ$_{27}$;f^{5}C$_{34}$ to have a significant effect on the binding of the ASL to AUG. As expected, steady-state binding assays of hmtASL$^{Met}_{CAU}$-Ψ$_{27}$;f^{5}C$_{34}$ or the hmtASL$^{Met}_{CAU}$-Ψ$_{27}$ to AUG at the P-site resulted in similar K_ds. However, there were differences in the levels of ASL concentration at which saturation was attained for the binding of AUG at the P-site, and also for AUA at the A-site (Fig. 7a,b). Thus, we explored the possibility that the two ASLs had significant differences in the kinetics of their binding. A significant difference in the kinetics of binding became apparent at a concentration of ASL (0.5 μM) far too low to saturate the ribosomes (Fig. 7c-d). The amount of hmtASL$^{Met}_{CAU}$-Ψ$_{27}$;f^{5}C$_{34}$ bound to AUG in the P-site was five-fold greater than that of the hmtASL$^{Met}_{CAU}$-Ψ$_{27}$ after only 30 seconds (Fig. 7). While the hmtASL$^{Met}_{CAU}$-Ψ$_{27}$ maintained a steady amount of weak binding over time, the amount of hmtASL$^{Met}_{CAU}$-Ψ$_{27}$;f^{5}C$_{34}$ bound to AUG continued to increase, reaching a ten-fold greater amount bound than that of the hmtASL$^{Met}_{CAU}$-Ψ$_{27}$ at the final time point of 30 min. These results were repeated for the binding of the two ASLs to AUG at the A-site, and AUA at both the P- and A-sites (Fig. 7). Though we were deterred in determining the rate constants for lack of sufficient modified hmtASL$^{Met}_{CAU}$, the time courses clearly indicate a significant difference in rates of association that are dependent on the presence of f^{5}C$_{34}$. The binding appears to be biphasic. We suspect that the 70S preparation has some portion of 30S subunits present. The subunits would form complexes rapidly accounting for an initial rapid phase in the kinetics. The slower phase may represent binding to 70S particles which probably takes longer either because access to the P-site is more restricted or because there is a dissociation step required in providing 30S subunits prior to the mRNA binding step. The equilibrium binding constants of the hmtASL$^{Met}_{CAU}$-Ψ$_{27}$ to the P-site codons AUG and AUA are not affected by the presence of f^{5}C$_{34}$ (Table 2), though there seems to be an effect on the extent of binding (Fig. 7). The similarities of the K_ds taken together with the results of the time courses at low ASL concentration indicate that the modification affects both on- and off- rates. In comparison, the equilibrium binding of the hmtASL$^{Met}_{CAU}$-Ψ$_{27}$ to the A-site codons AUG and AUA is enhanced by the presence of the f^{5}C$_{34}$, and the respective time courses reflect this result. This suggests that in the absence of f^{5}C, the off-rate may predominate.

Codon binding of hmtASL$^{Met}_{CAU}$-Ψ$_{27}$;f^{5}C$_{34}$ and the hmtASL$^{Met}_{CAU}$-Ψ$_{27}$ on the bovine 55S mitochondrial ribosome

Thus far, the codon binding experiments we have described for hmtASL$^{Met}_{CAU}$ were conducted with the model *E. coli* 70S ribosomes. However, previous studies of translation *in vitro* using bovine mitochondrial 55S ribosomes succeeded in demonstrating low levels of incorporation of methionine into protein using the native bovine mtRNA$^{Met}_{CAU}$, unmodified transcripts and mitochondrial ribosomes programmed with poly(AUA).[14] Therefore, we thought it appropriate to attempt the binding of hmtASL$^{Met}_{CAU}$ to programmed, purified bovine mitochondrial 55S ribosomes. The bovine mitochondrial 55S ribosomes were programmed with mRNA, and then either hmtASL$^{Met}_{CAU}$-Ψ$_{27}$;f^{5}C$_{34}$ or the hmtASL$^{Met}_{CAU}$-Ψ$_{27}$ was added. Mitochondrial mRNAs tend to lack the 5′-UTR. In order to study the binding of hmtASL$^{Met}_{CAU}$ to the initiation site (P-site), we used a 30-mer

oligonucleotide mRNA with either AUG or AUA at the 5′ terminal end followed by the valine codon GUA as the second codon. The binding of the ASLs to AUG in the P-site was detectable, although the level of codon binding was considerably lower than that observed on the *E. coli* ribosomes. The 5-formyl-group of the f^5C_{34}-modified $hmtASL^{Met}_{CAU}$ enhanced the binding of AUG by approximately 40% (Fig. 8a, first two bars). Though the P-site binding of the $hmtASL^{Met}_{CAU}$-Ψ_{27};f^5C_{34} to AUA was detectable, the binding of the $hmtASL^{Met}_{CAU}$-Ψ_{27} was not (Fig. 8a, second two bars). The presence of f^5C_{34} appears to have enhanced P-site binding. To observe A-site binding, the 55S ribosomes were programmed with a 30-mer mRNA construct consisting of a 5′-leader of twelve uridines, followed by GUA at the P-site and AUG or AUA at the A-site, and ending with another stretch of twelve U residues. The presence of the 5-formyl modification on the ASL enhanced A-site binding to AUG sufficiently for it to be observed (Fig. 8a). However, neither the binding of $hmtASL^{Met}_{CAU}$-Ψ_{27} to AUG, nor the binding of either ASL to AUA was observed in the A-site.

In our mitochondrial 55S ribosome binding assays, only small amounts of the $hmtASL^{Met}_{CAU}$-Ψ_{27};f^5C_{34} bound AUG at the A-site and AUA at the P-site. The low level of detectable binding to the P-site, and the inability to detect the binding of either $hmtASL^{Met}_{CAU}$-Ψ_{27};f^5C_{34} or the unmodified $hmtASL^{Met}_{CAU}$ to AUA at the A-site may have been due to the very low levels of binding to mitochondrial ribosomes, in general, experienced by us (approximately 0.8 pmol of $hmtASL^{Met}_{CAU}$-Ψ_{27};f^5C_{34} bound to AUG at the P-site) and others[10,14] in comparison to *E. coli* 70S ribosomes (4 pmol of $hmtASL^{Met}_{CAU}$-Ψ_{27};f^5C_{34} bound to AUG at the P-site[10]). Also, the codon AUA is not as efficient as AUG in the decoding of methionine in mitochondrial translation. Translation *in vitro* with a poly(AUG) mRNA resulted in five-fold greater amounts of Met-containing polypeptides being produced than from a poly(AUA) mRNA.[14]

The lack of full tRNAs, aided by initiation and elongation factors, may also have contribute to the low levels of binding. Therefore, we conducted initiation factor, $IF2_{mt}$-facilitated, binding of the native bovine $mtRNA^{Met}_{CAU}$ and the full length, but unmodified, transcript to codons at the P-site of the bovine mitochondrial 55S ribosome. Native bovine $mtRNA^{Met}_{CAU}$ was isolated and purified,[29] and the unmodified $mtRNA^{Met}_{CAU}$ obtained through transcription *in vitro*.[30] The native tRNA and transcript were aminoacylated and formylated. The IF-2_{mt}-facilitated binding of the native bovine and unmodified transcript of fmet-$mtRNA^{Met}_{CAU}$ to AUG at the P-site were essentially identical at very low levels of input tRNA (Fig. 8b). The affinity of the two tRNAs for AUA at the P-site was considerably lower. However, the absence of modifications on the transcript made no apparent difference in the binding. Thus, the binding of full length native bovine fMet-$mtRNA^{Met}_{CAU}$ and the unmodified transcript to AUG at the P-site of the mitochondrial ribosome was consistent with the results obtained in the binding of the $hmtASL^{Met}_{CAU}$-Ψ_{27};f^5C_{34} and $hmtASL^{Met}_{CAU}$-Ψ_{27}. Though the fMet-$mtRNA^{Met}_{CAU}$ and the unmodified transcript comparably bound AUA at the P-site, the extent was diminished to the degree as to not be able to make a reasonable comparison to the binding of the respective mtASLs. The mitochondria uses AUA to initiate translation (AUA at the P-site) only about twenty percent of time, but approximately eighty percent of mitochondrial methionine A-site codons are AUA (twenty percent are AUG).[21,31] Thus, the probability of AUA being at the mitochondrial P-site is significantly lower than that of AUG.

Ability of the 5-formyl-modification to expand codon recognition within the codon box AUN

Mitochondria not only initiate translation from AUG and AUA, but also have been found to initiate from the two mitochondrial isoleucine codons AUU and AUC.[9,24,32] AUU and AUC are rare initiation codons and may be used to regulate gene expression. The ability of this

single and modest modification, f^5C_{34}, to enable the one hmtRNA$^{Met}_{CAU}$ to initiate translation with AUA, as well as with AUG, begs the question as to whether f^5C_{34} expands the tRNA's ability to decode the other synonymous codons, AUU and AUG. We found that the hmtASL$^{Met}_{CAU}$-Ψ_{27};f^5C_{34} bound to AUU and to AUC with a K_d similar to that for AUA (Fig. 9). Furthermore, as it did in binding to AUA, the modified hmtASL$^{Met}_{CAU}$-Ψ_{27};f^5C_{34} bound to AUU and AUC with a dissociation constant that was two- to three-fold less than that of the hmtASL$^{Met}_{CAU}$-Ψ_{27} (Fig. 9). The hmtASL$^{Met}_{CAU}$-Ψ_{27} was bound to AUU, AUC, and AUA with K_ds comparable to, and within error of, that of the negative-control codon for valine GUA (Fig. 9).

Discussion

Determining the structural contributions of f^5C_{34} to the function of mtRNA$^{Met}_{CAU}$ presented a unique challenge because this single RNA has the dual role of participating in initiation and elongation, as well as reading both AUA and AUG. The hmtRNA$^{Met}_{CAU}$ has unique decoding properties because the f^5C_{34} extends codon recognition often to AUA, and to a small extent to AUU and AUC. The hmtASL$^{Met}_{CAU}$-Ψ_{27};f^5C_{34} and hmtASL$^{Met}_{CAU}$-Ψ_{27} exhibited the same overall conformation expected of a hairpin RNA with a stem adopting an A-form RNA structure extended by a non-canonical base pair between C_{32}●C_{38}. The 5′ side of the loop was characterized by the stacking of C_{32} with the unique C_{33}, and the 3′ side by the stacking of A_{35}, A_{37} and C_{38}. A sharp turn was observed in the backbone and was characterized by a *trans* α dihedral angle between the residues C_{33} and f^5C_{34}/C_{34}. This observation is in accordance with the downfield ^{31}P resonance belonging to f^5C_{34}/C_{34} and represents one of the characteristics of the U-turn motif.[33,34] Moreover, the "classical" U-turn motif is stabilized by a network of hydrogen bonds between the U_{33}2′OH and the N7 of the purine at residue 35 (most often an adenosine), and by a hydrogen bond between the U_{33}H3 exchangeable proton and the phosphate group of residue 36. These hydrogen bonds have been shown to be essential in the formation of the U-turn and to the ribosomal binding properties of the tRNAs.[35] Because C_{33} substitutes for the invariant U_{33}, some of the hydrogen bonds that stabilize the canonical U-turn conformation adopted by cytoplasmic tRNA$^{Met}_{CAU}$ and other tRNAs should not be possible for the hmtRNA$^{Met}_{CAU}$.[33,35] The last hydrogen bond is not possible in the case of a cytosine in position 33, unless the amino group of the cytosine plays the role of hydrogen bond donor. The three dimensional structures of the hmtASL$^{Met}_{CAU}$-Ψ_{27};f^5C_{34} and the hmtASL$^{Met}_{CAU}$-Ψ_{27} showed that the C_{33} amino group is directed toward the minor groove and is not involved in direct hydrogen bonding. Nevertheless, distances between the C_{33}N4 and the O2P of residue C_{32} are on average 4.07 ± 0.72 Å and 3.93 ± 0.55 Å for hmtASL$^{Met}_{CAU}$-Ψ_{27};f^5C_{34} and hmtASL$^{Met}_{CAU}$-Ψ_{27}. If these distances preclude the formation of a direct hydrogen bond, the formation of some indirect hydrogen bonds involving water molecules is highly possible. Water mediated hydrogen bonds can be of importance in the stabilization of the loop conformation and the formation of the observed ersatz U-turn, or "C-turn". The projection of the U_{36} residue from the structure and into the solvent is consistent with the NMR data. This is not very surprising when we consider that the uridine is unpaired and between the two stacked purines, A_{35} and A_{37}. Unpaired uridines have a tendency to bulge from the structure.[34] Modifications in position 37 provide stability to the anticodon-codon interaction,[36] and are important in driving the conformation of the anticodon loop toward that of the well-known U-turn important to the binding of the codon on the ribosome.[37–39] In the anticodon domain structure of the *S. pombe* initiator tRNA$^{Met}_{CAU}$, with a uridine in position 33 and the t^6A_{37} modified residue, U_{36} is also bulged out from the structure,[38] whereas in the structure of the unmodified yeast initiator tRNA^{Met}, U_{36} adopted the *C2′-endo* sugar conformation and is loosely stacked with A_{35}.[41] Direct exposure of U_{36} to the solvent makes it available for tertiary interactions, in particular with the mitochondrial methionyl-tRNA^{Met} synthetase (mtMRS). mtMRS recognition of the cytoplasmic tRNA^{Met} species includes the

anticodon,[42],[43] and especially residue C_{34} as a strong identity element.[44] Moreover, the residue U36 has been shown to be essential for the $tRNA^{Met}$ – MetRS interaction by being specifically recognized by the MetRS C-terminal extended loop.[45]

The f^5C_{34} modified residue is one of the most conformationally rigid residues with a *C3′-endo* sugar conformation that could help in pre-structuring the anticodon for codon interaction.[39],[46] Yet, UV-monitored studies of thermal stability and circular dichroism studies of stacking interactions of the $hmtASL^{Met}_{CAU}$-Ψ_{27} with and without f^5C_{34} indicated that the introduction of f^5C_{34} may enhance the ASL's motional dynamics.[15] While the biological function of f^5C_{34} is evident from our work and that of others, the physicochemical contribution of the f^5C_{34} distinguishing $hmtASL^{Met}_{CAU}$-Ψ_{27};f^5C_{34} from $hmtASL^{Met}_{CAU}$-Ψ_{27} appears ambiguous. However, this apparent contradiction of thermal instability and restricted conformational dynamics is found in other ASLs when the introduction of a modified nucleoside at positions 34 and/or 37 increases the width of the anticodon loop, as does f^5C_{34}.[47] As with other wobble position-34 modifications,[37],[48],[49] the f^5C_{34} also takes a defined chemical and physical space within the anticodon loop that possibly restricts the conformational dynamics of the other loop nucleosides, in particular A_{35} and A_{37}, in comparison to that of $hmtASL^{Met}_{CAU}$-Ψ_{27} (Fig. 5). In the absence of stable isotope labeling, the restricted dynamics are deduced from a comparison of the family of calculated structures for $hmtASL^{Met}_{CAU}$-Ψ_{27};f^5C_{34} with that of $hmtASL^{Met}_{CAU}$-Ψ_{27} (Fig. 5) We suggest that the mechanism by which the formyl oxygen of f^5C_{34} may restrict conformational dynamics is similar to that of the C5-oxygen of 5-oxyacetic acid uridine (cmo^5U_{34}). Cmo^5U_{34}, found in one of the isoaccepting species for each of the *E. coli* tRNAs for alanine, proline, threonine, serine and valine, enables the tRNA's reading of all four synonymous codons by pre-structuring of the anticodon, and fixing the geometry of the base in the A-site of the ribosome.[48];[49]

Position-37 is not modified in the $mtRNA^{Met}_{CAU}$. Modifications of the purine at position-37 provide stability to the tRNA/mRNA interactions, and have been shown to be important in driving the conformation of the ASL toward the well-known U-turn structure that accommodates the binding to cognate codons on the ribosome.[39],[47] The presence of a cytosine in position-33 is quite unusual.[16] Of the 21 sequences of tRNAs having a cytosine in position-33, 12 are cytoplasmic initiator $tRNAi^{Met}_{CAU}$ and three are mitochondrial $mtRNA^{Met}_{CAU}$.[16] Surprisingly, the presence of a cytosine residue in position-33 is correlated with the absence of modifications in position-37 in mitochondria, except for that of plants. The structures of the two cytoplasmic $tRNA^{Met}_{CAU}$ species have been studied. Crystal structures have been solved for the entire eukaryotic yeast and *E. coli* $tRNA^{Met}_{CAU}$ species free,[50]-[53] and in complex with the methionyl-tRNA synthetase (metRS).[54] In addition, the anticodon stem and loops of the *E. coli* $tRNA_f^{Met}_{CAU}$ and unmodified $tRNA_m^{Met}_{CAU}$ were solved by NMR,[41] as well as that of the *S. pombe* $tRNA^{Met}_{CAU}$ ASL containing the t^6A_{37} modification.[38] The anticodon stem and loop domains of yeast, *E. coli*, human and plant initiator tRNAs have the same primary sequence (residues 29-41) except for position-33 which is a uridine in yeast and *E. coli* initiator tRNAs, and a cytosine in human and plant initiator tRNAs. This singular difference appears to be responsible for the specific, H_2O-mediated hydrolysis of the C_{34}-A_{35} phosphodiester bond in human and plant initiator tRNAs, and not in yeast and *E. coli* initiator tRNAs.[55] The substitution of U_{33} with C_{33} in elongating tRNAs has been shown to decrease codon binding on the ribosome.[35],[56] Substitution of U_{33} for C_{33} in $hmtASL^{Met}_{CAU}$ does not affect P-site binding to either AUG or AUA (not shown). Nevertheless, the S1 nuclease cleavage patterns for the anticodon stem and loop domains of the prokaryotic and eukaryotic initiator tRNAs remain the same whether a cytosine or a uridine is in position-33.[57]

The A-site anticodon/mRNA interaction is proof-read and stabilized by the 16S rRNA residues G_{530}, A_{1492} and A_{1493}.[58] Crystal structures of the ribosome show that U_{33} does not make contact with the ribosome, and that the U_{33}N3 is involved in the "classical" U-turn hydrogen bond.[18,36] In the NMR structures of the hmtASL$^{Met}_{CAU}$, C_{33} lacks that hydrogen bond. Once on the ribosome, the amino group of C_{33} is available to form tertiary interactions with the rRNA that could stabilize the anticodon/codon binding. Interestingly, the crystal structure mentioned above reveals that the anticodon P-site tRNA^{Phe} wobble base (G_{34}) is stabilized by stacking interactions with the 16S rRNA base C_{1400} and by packing between the ribose of G_{34} and the base G_{966}.[59] If the same interactions are observed in the case of the hmtRNA$^{Met}_{CAU}$, the enhanced stacking properties of the f^5C_{34} modified residue could account for stabilization of the hmtASL^{Met}/mRNA interaction. It appears that the C_{33} may change the conformational dynamic of the ASL loop, and thus could be of importance in stabilizing the f^5C●A base pair, as well as that with AUG.

A pre-structured anticodon is the result of modification-induced, restricted dynamics, and is advantageous for codon binding.[39] The three hydrogen bonds between an f^5C_{34} and a guanosine are no different than that of a tRNA's C_{34}●G base pair with the mRNA codon. However, codon recognition and binding of the hmtRNA$^{Met}_{CAU}$ to AUA in the P- or A-sites is problematic because the unconventional f^5C_{34}●A interaction would be expected to be quite weak.[60] Yet, eighty percent of all methionine codons internal to mitochondrial mRNAs are AUA. We have found that that the f^5C_{34} facilitates the binding of the hmtASL$^{Met}_{CAU}$-Ψ_{27};f^5C_{34} at the A-site, and also may effect the kinetics of codon recognition at both the P- and A-sites. In addition, humans, giant pandas and fruit flies have been found to use AUU for initiation with methionine, honey bees use AUC, and mice use both AUU and AUC to initiate translation.[24,25] The hmtASL$^{Met}_{CAU}$-Ψ_{27};f^5C_{34} read AUU and AUC at the P-site to an extent similar to its binding to AUA, whereas the hmtASL$^{Met}_{CAU}$-Ψ_{27} was not able to do so. Thus, the f^5C_{34} appears to have expanded the ability of the tRNA to read all four synonymous codons within the AUN codon box.

Molecular dynamics simulations of the base pairing of the 5′-monophosphate of f^5C_{34} with that of A under aqueous and neutral conditions[61] indicate the potential for novel interactions, including a bridging H_2O molecule that stabilizes the interaction (Fig. 10). The f^5C_{34} intranucleotide hydrogen bond that we observed between the f^5C_{34} amino and formyl groups in the NMR-derived structure could increase the stacking interaction between f^5C_{34} and A_{35} and possibly A_{37}, and thus compensate for the lack of hydrogen bonds in an anticodon f^5C●A codon interaction.[14] A hydrogen bond between the N4-amino group and the formyl-group oxygen at the position C5 of the f^5C_{34} modification may have altered the electronic properties of the modified residue, and thereby affected the base pairing properties of the f^5C_{34}, enabling a f^5C_{34}●A mismatch to form on the ribosome, as it has been proposed.[14] An additional hydrogen-bond could be formed between f^5C_{34} of the anticodon and A, the third base of the codon, if the adenosine were protonated. This is possible since protonation of an adenosine has been shown to be effective in certain RNA constructs at a pH near 7.[62] Nevertheless, an f^5C●A^+ interaction is still weaker than an f^5C●G or C●G interaction. Further studies need to be conducted to reveal the geometry, and stability that the f^5C_{34} modification brings to the interactions of the hmtRNA^{Met} with unconventional codons of mRNA in the A- and P-sites of the ribosome.

Materials and Methods

Oligonucleotide Chemical Synthesis and tRNA Preparation

RNAs were chemically synthesized (Thermo Fisher Scientific, Lafayette, CO) using "ACE" chemistry.[63] The protected 5-formylcytidine modified nucleotide was chemically synthesized and incorporated at position-34.[15] The RNA molecules were deprotected and

dialyzed extensively against 20 mM phosphate buffer (10 mM KH_2PO_4; 10 mM Na_2HPO_4; pH 6.8; 0.05 mM EDTA) using a membrane with a 3500 Da cutoff. For observation of the exchangeable protons by NMR, the samples were resuspended in 300 μl of 90% H_2O/10% D_2O. For experiments involving the non-exchangeable protons, the samples were exchanged twice with 99.9% D_2O. The NMR sample concentration was between 1.0 and 1.5 mM. Full length, native bovine $mtRNA^{Met}_{CAU}$ and its unmodified transcript were prepared as previously described.[30]

NMR Spectroscopy

NMR spectra were collected on a DMX Bruker 500 MHz instrument equipped with a triple-resonance ^{1}H, ^{13}C, and ^{15}N probe and three-axis pulsed field gradient capabilities, and on a Varian INOVA 600 MHz instrument equipped with a cryoprobe. NMR spectra were collected with the RNA samples under solution and temperature conditions required and widely used for determination of nucleic acid structures.[49],[62],[64] All NMR data were processed using NMRPIPE.[65] Spectra were displayed and analyzed using SPARKY software.[66] NOESY spectra in D_2O were recorded at 10, 25 and 30° C with mixing times of 50, 150 and 400 ms. TOCSY, COSY and DQF-COSY experiments were acquired at 25 °C. Natural abundance ^{1}H-^{13}C HSQC and ^{1}H-^{31}P HETCOR experiments were recorded in D_2O at 25 °C. For the study of exchangeable protons, 1D 1H and 2D NOESY spectra were recorded at different temperatures with various mixing time using the Watergate water suppression sequence. In confirmation of the unimolecular character of the ASLs after purification and dialysis, 1D 1H and 1D-^{31}P spectra were recorded immediately. The ^{31}P NMR spectrum exhibited a highly downfield resonance (characteristic of the canonical U-turn conformation) that we attributed to be P_{34}. This property was confirmed with the ^{31}P resonance assignments using the ^{31}P-1H HECTOR NMR spectrum. Other assignments confirmed that we had a C-turn (a pseudo-like U-turn). For both RNAs (with or without the f^5C_{34} modification), a dipolar connectivity between the protons A_{35}-H8/C_{33}-H1′ was observed within the NOESY spectra also characteristic of the canonical U-turn (Fig. 3). The formation of a C-turn is incompatible with the RNA adopting a duplex conformation. A duplex conformation would probably result in non-canonical, mismatch base pairs between C_{32}-C_{38}, C_{33}-A_{37} and others. In a duplex conformation, observation of the A_{35}-H8/C_{33}-H1′ dipolar connectivity would require the flipping out of the residue f^5C_{34}. This was absolutely not the case as we observed NOE connectivities between the residues f^5C_{34} and A_{35} (C_{34}/f^5C_{34}-H6/A_{35}-H8 and between f^5C_{34} H7–A_{35} H8) demonstrating that those two residues are stacked.

NMR restraints generation and structure calculation

NMR data collected at 25° and 30° C were used for the structure calculations. The NOE cross-peaks were integrated using the peak fitting Gaussian function and volume integration in SPARKY software. Using the intensity of the cross peak, and as reference the H5-H6 covalent distance for uridine and cytosine residues, the cross-peaks were qualitatively classified as strong (3.0 1.2 0.0), medium strong (4.0 2.0 0.0), medium (5.0 3.0 0.0), weak (5.0 2.0 0.0) or very weak (6.0 3.0 0.0). No inter-nucleotide restraints were used from the H5′ and H5″ protons. For restraints involving imino protons, (3.0 1.2 0.0) and (5.0 3.0 0.0) intervals were used. A total number of 266 and 275 distance restraints were employed for generating the structures of the $hmtASL^{Met}_{CAU}$-Ψ_{27};f^5C_{34} and the $hmtASL^{Met}_{CAU}$-Ψ_{27} (Table 2). Consistent with the NMR data, the four stem G●C Watson-Crick base pairs were subjected to six hydrogen-bond restraints (1.8-2.5 Å between the donated hydrogen and the acceptor, and 2.7 - 3.5 Å between the two heavy atoms). No hydrogen bond restraints were used between Ψ_{27} and A_{43}, despite the observation of an NOE between the Ψ_{27}H3 imino proton and the A_{42}NH2 protons. Dihedral constraints on the ribose ring and backbone were derived from semi-quantitative measurement of the $^{3}J_{H\text{-}H}$ and $^{3}J_{H\text{-}P}$ couplings. Sugar pucker

conformations were derived from the observation of the COSY and DQF-COSY spectra. Due to the large U_{36}H1′-H2′ coupling observed, this residue was constrained to the *C2′-endo* (δ: 160 ± 20°), whereas for the other residues only weak (A_{43}) or very weak H1′-H2′ connectivity was observed on the COSY spectra and these residues were therefore, left unrestrained (A_{43}) or constrained to the *C3′-endo* conformation (δ: 85 ± 20°). Independent confirmation of the U_{36} sugar pucker conformation was derived from the ^{1}H-^{13}C HSQC spectra, and the C3′ and C4′ resonances downfield from the main cluster of sugar resonances. The **γ** torsion angle was derived from the $^{3}J_{H4'\text{-}H5'}$ and $^{3}J_{H4'\text{-}H5''}$ peaks in the COSY and DQF-COSY. For residues that lacked H4′-H5′ and H4′-H5″ peaks (J < 5Hz), **γ** was constrained to the g^{+} conformation (54 ± 20°). For the other residues, **γ** was left unrestrained. **β** dihedral angles were derived from the $^{3}J_{P\text{-}H5'}$ and $^{3}J_{P\text{-}H5''}$ couplings observed in the ^{1}H-^{31}P HETCOR NMR spectrum. When the $^{3}J_{P\text{-}H5'}$ and $^{3}J_{P\text{-}H5''}$ were clearly absent, **β** was constrained to the *trans* conformation (178 ± 20°). When $^{3}J_{P\text{-}H5'}$ and $^{3}J_{P\text{-}H5''}$ could be observed, **β** was left unrestrained. All H3′-P were clearly identified on the ^{1}H-^{31}P HETCOR (^{3}J > 5Hz), so the **ε** dihedral angle were loosely constraint to avoid the steric forbidden g^{+} conformation (-120 ± 120°). Dihedral angle restraints for the **α** and **ζ** were derived from the observation of the ^{31}P chemical shifts. All of the ^{31}P resonances, except for ^{31}P of the $f^{5}C_{34}$ and C_{34} which were found strongly downfield and A_{37} to a lesser extent, were in a sharp range of chemical shift. The U_{36} ^{31}P chemical shift was upfield to the majority of the ^{31}P resonances. Thus, **α** and **ζ** were constraints to avoid the *trans* conformation resulting in strongly downfield 31P resonances (0 ± 120°). F_5C_{34}/C_{34}, A_{37} and U_{36} α and ζ dihedral angles were left unrestrained. Each of the intra-aromatic to H1′ NOE connectivities of the different ASL residues had an intensity significantly less than that for the H5-H6 NOE connectivity showing that all the bases adopted an *anti* glycosidic torsional angle. Thus, the **χ** glycosidic dihedral angle was constrained to the *anti* conformation for all residues. NMR restrained molecular modeling of the hmtASL$^{Met}_{CAU}$-Ψ_{27};f^{5}C and hmtASL$^{Met}_{CAU}$-Ψ_{27} structures was achieved using CNS 1.2.[67,68] One hundred structures were calculated using a standard NMR restrained annealing protocol.[69] The 10 structures having the lowest total energy, without dihedral or distances restraint violations, were chosen for further analysis. The structure helical parameters were analyzed using X3DNA software.[70] The output structures were visualized with MOLMOL and PYMOL.[71]

Codon Binding

In order to observe binding at the P-site, ribosomes were programmed with a 27-mer oligonucleotide mRNA containing a Shine-Dalgarno sequence at the 5′-leader, an AUG or AUA at the P-site, and the valine codon GUA at the A-site. The binding of mRNA was assessed using radiolabeled mRNAs to ensure that the different mRNAs were bound by the ribosome similarly. The binding of the different mRNA sequences to the ribosomes revealed no significant differences (data not shown). Since ASLs bind P-site codons significantly better (~100-fold) than A-site codons[27] and both the hmtASL$^{Met}_{CAU}$-Ψ_{27};$f^{5}C_{34}$ and hmtASL$^{Met}_{CAU}$-Ψ_{27} bound the valine codon GUA poorly in the A- or P-sites, similar to that of nonspecific ribosome binding (data not shown), the A-site was left empty. Near saturation, the amount of hmtASL$^{Met}_{CAU}$-Ψ_{27};$f^{5}C_{34}$ and hmtASL$^{Met}_{CAU}$-Ψ_{27} bound to AUG in the P-site exceeded their binding of AUG in the A-site by many fold (2-4 pmoles bound compared to 0.5-1.0 pmoles). In order to study the binding of the hmtASLs to the A-site codons AUG or AUA, the *E. coli* 70S ribosome was programmed with a 27-nucleotide mRNA with a 5′-leader with containing the Shine-Dalgarno sequence, the Val codon GUA at the P-site, and either AUG or AUA at the A-site. The P-site was saturated with unmodified ASL$^{Val}_{UAC}$ and A-site binding by either hmtASL$^{Met}_{CAU}$-Ψ_{27};$f^{5}C_{34}$ or the hmtASL$^{Met}_{CAU}$-Ψ_{27} was tested. Control experiments saturating the GUA-programmed A-site with ASL$^{Val}_{UAC}$ after P-site binding revealed similar results as those in the absence of ASL$^{Val}_{UAC}$ (data not shown). The 70S ribosomal subunits were prepared from *E. coli*

MRE600.[72] Insignificant amounts of the ASLs that had been 5′-endlabeled with ^{32}P using [γ-^{32}P] ATP (MP Biomedicals)[15], and were radiochemically detectable (2,000-5,000 CPM), were mixed in a fixed ratio with unlabeled ASLs in a range of concentrations (0-5 μM).[49] The filter binding assay (30 min; 25 °C) was performed with activated ribosomes (0.25 μM; 5 pmoles) that had been programmed with mRNA (2.5 μM) and used the ribosomal binding buffer (50 mM HEPES, pH 7.0; 30 mM KCl; 70 mM NH_4Cl; 1 mM DTT; 100 μM EDTA; 20 mM $MgCl_2$).[49] Data collected from a phosphoimager were measured for radioactive intensity using ImageQuant (Amersham). Nonspecific binding was determined by the binding of ASLs to ribosomes without mRNA and subtracted from the experimental data. In general, the final data is a result of at least three separate experiments, each done with samples in triplicate, ie. minimally nine determinations for each binding with the result in the absence of mRNA subtracted. Data were analyzed using single-site, nonlinear regression (Prism, GraphPad Software, Inc., San Diego, CA).[49] Dissociation constants (K_ds) were extracted from the binding curves.

Ribosomal Kinetic Assays

The kinetic assays were conducted in a similar fashion as the ribosomal binding assays described above with the exception that only a single low concentration of ASL was used (0.5 μM) and binding was monitored on a time course. Aliquots of ribosomal reactions were filtered after: 0.0, 0.25, 0.5, 1, 5, 10, 15, 20, 30 minutes. The nitrocellulose was washed, dried, and processed as described.

Bovine Mitochondrial 55S Binding Assays

Bovine mitochondrial, 55S, ribosomes were isolated and purified as previously described.[10] Bovine 55S mitochondria were programmed with a chemically synthesized 30-mer oligonucleotide. Mammalian mitochondrial mRNAs are leaderless and translation initiation begins at the first nucleoside triplet on the mRNA. Therefore, to study binding at the P-site, we designed the mRNAs (see the following sequences) with an AUG or AUA (in bold) as the first three nucleosides, followed by the valine codon GUA (underlined) at the A-site, and a stretch of poly-Uridines:

1. 5′-**AUG**GUAUUUUUUUUUUUUUUUUUUUUUU-3′
2. 5′-**AUA**GUAUUUUUUUUUUUUUUUUUUUUUU-3′.

The mRNAs of mammalian mitochondria do not consist of a ribosomal binding sequence such as the Shine-Dalgarno sequence found in bacterial mRNAs. However, an mRNA consisting of stretches of poly(U) with the mitochondrial methionine codon AUG has been shown to be successful in translating methionine using an mitochondrial translational system *in vitro*.[10,14] Therefore, this poly(U)-methionine codon mRNA can be incorporated into the mitochondrial 55S ribosome. To study the binding of the hmtASL$^{Met}_{CAU}$-Ψ_{27};f^5C_{34} to the A-site, we incorporated the valine codon GUA (intended for the P-site; underlined in the following mRNA sequences), followed by AUG or AUA (in bold) into a string of 24 Uridines:

1. 5′-UUUUUUUUUUUU<u>GUA</u>**AUG**UUUUUUUUUUUU-3′
2. 5′-UUUUUUUUUUUU<u>GUA</u>**AUA**UUUUUUUUUUUU-3′.

Full length, native bovine mtRNA$^{Met}_{CAU}$ and its transcript were aminoacylated and formylated.[14] The IF2-facilitated binding of the full length tRNAs to AUG and AUA in the P-site was conducted as previously described.[73,74]

Acknowledgments

The authors would like to thank William Cantara for critical reading of the manuscript. This work was supported by grants from the National Institutes of Health and the National Science Foundation to P.F. A. (2RO1-GM23037 and MCB0548602, respectively), by National Institutes of Health grant GM32734 to L.L.S. and from the United Mitochondrial Disease Foundation to L.L.S, and P.F.A. (05-20), and by Dharmacon-Thermo Fisher Scientific.

Abbreviations

f^5C_{34}	5-formylcytidine at position 34
ASL	anticodon stem and loop
NOE	nuclear Overhauser effect
NOESY	nuclear Overhauser spectroscopy
COSY	correlation spectroscopy
TOCSY	total correlation spectroscopy
HSQC	heteronuclear single quantum correlation
RNA	ribonucleic acids
tRNA	transfer ribonucleic acids
mRNA	messenger RNA
ppm	part per million
RMSD	root mean square deviation
NMR	nuclear magnetic resonance

References

1. Anderson S, Bankier AT, Barrell BG, de Bruijn MH, Coulson AR, Drouin J, Eperon IC, Nierlich DP, Roe BA, Sanger F, Schreier PH, Smith AJ, Staden R, Young IG. Sequence and organization of the human mitochondrial genome. Nature. 1981; 290:457–465. [PubMed: 7219534]
2. Aujame L, Freeman KB. Mammalian mitochondrial transfer RNAs: chromatographic properties, size and origin. Nucleic Acids Res. 1979; 6:455–469. [PubMed: 424302]
3. Rubio MA, Rinehart JJ, Krett B, Duvezin-Caubet S, Reichert AS, Söll D, Alfonzo JD. Mammalian mitochondria have the innate ability to import tRNAs by a mechanism distinct from protein import. Proc Natl Acad Sci USA. 2008; 105:9186–9191. [PubMed: 18587046]
4. Tomita K, Ueda T, Ishiwa S, Crain PF, McCloskey JA, Watanabe K. Codon reading patterns in Drosophila melanogaster mitochondria based on their tRNA sequences: a unique wobble rule in animal mitochondria. Nucleic Acids Res. 1999; 27:4291–4297. [PubMed: 10518623]
5. Santos MA, Moura G, Massey SE, Tuite MF. Driving change: the evolution of alternative genetic codes. Trends Genet. 2004; 20:95–102. [PubMed: 14746991]
6. Temperley R, Richter R, Dennerlein S, Lightowlers RN, Chrzanowska-Lightowlers ZM. Hungry codons promote frameshifting in human mitochondrial ribosomes. Science. 2010; 327:301. [PubMed: 20075246]
7. Young IG, Anderson S. The genetic code in bovine mitochondria: sequence of genes for the cytochrome oxidase subunit II and two tRNAs. Gene. 1980; 12:257–65. [PubMed: 6265319]
8. Anderson S, de Bruijn MH, Coulson AR, Eperon IC, Sanger F, Young IG. Complete sequence of bovine mitochondrial DNA. Conserved features of the mammalian mitochondrial genome. J Mol Biol. 1982; 156:683–717. [PubMed: 7120390]
9. Fearnley IM, Walker JE. Initiation codons in mammalian mitochondria: differences in genetic code in the organelle. Biochemistry. 1987; 26:8247–8251. [PubMed: 2964865]

10. Takemoto C, Koike T, Yokogawa T, Benkowski L, Spremulli LL, Ueda TA, Nishikawa K, Watanabe K. The ability of bovine mitochondrial transfer RNA^{Met} to decode AUG and AUA codons. Biochimie. 1995; 77:104–108. [PubMed: 7599268]
11. Crick FH. Codon--anticodon pairing: the wobble hypothesis. J Mol Biol. 1966; 19:548–555. [PubMed: 5969078]
12. Björk, GR. Biosynthesis and function of modified nucleosides. In: Söll, D.; Rajbhandary, UL., editors. tRNA: Structure, Biosynthesis, and Function. ASM Press; Washington, D.C: 1995. p. 165-206.
13. Moriya J, Yokogawa T, Wakita K, Ueda T, Nishikawa K, Crain PF, Hashizume T, Pomerantz SC, McCloskey JA, Kawai G, Hayashi N, Yokoyama S, Watanabe K. A novel modified nucleoside found at the first position of the anticodon of methionine tRNA from bovine liver mitochondria. Biochemistry. 1994; 33:2234–2239. [PubMed: 7509636]
14. Takemoto C, Spremulli LL, Benkowski LA, Ueda T, Yokogawa T, Watanabe K. Unconventional decoding of the AUA codon as methionine by mitochondrial tRNA^{Met} with the anticodon f^{5}CAU as revealed with a mitochondrial in vitro translation system. Nucleic Acids Res. 2009; 37:1616–1627. [PubMed: 19151083]
15. Lusic H, Gustilo EM, Vendeix FA, Kaiser R, Delaney MO, Graham WD, Moye VA, Cantara WA, Agris PF, Deiters A. Synthesis and investigation of the 5-formylcytidine modified, anticodon stem and loop of the human mitochondrial tRNA^{Met}. Nucleic Acids Res. 2008; 36:6548–6557. [PubMed: 18927116]
16. Jühling F, Mörl M, Hartmann RK, Sprinzl M, Stadler PF, Pütz J. tRNAdb 2009: compilation of tRNA sequences and tRNA genes. Nucleic Acids Res. 2009; 37:D159–D162. Database issue: http://trnadb.bioinf.uni-leipzig.de/. [PubMed: 18957446]
17. Takemoto C, Ueda T, Miura K, Watanabe K. Nucleotide sequences of animal mitochondrial tRNAs(Met) possibly recognizing both AUG and AUA codons. Nucleic Acids Symp Ser. 1999; 42:77–78. [PubMed: 10780387]
18. Watanabe Y, Tsurui H, Ueda T, Furushima R, Takamiya S, Kita K, Nishikawa K, Watanabe K. Primary and higher order structures of nematode (*Ascaris suum*) mitochondrial tRNAs lacking either the T or D stem. J Biol Chem. 1994; 269:22902–22906. [PubMed: 8077242]
19. Tomita K, Ueda T, Watanabe K. 5-formylcytidine (f^{5}C) found at the wobble position of the anticodon of squid mitochondrial tRNA^{Met}CAU. Nucleic Acids Symp Ser. 1997:197–198. [PubMed: 9586067]
20. Jones CN, Jones CI, Graham WD, Agris PF, Spremulli LL. A disease-causing point mutation in human mitochondrial tRNA^{Met} results in tRNA misfolding leading to defects in translational initiation and elongation. J Biol Chem. 2008; 283:34445–34456. [PubMed: 18835817]
21. Jones CN, Wilkinson KA, Hung KT, Weeks KM, Spremulli LL. Lack of secondary structure characterizes the 5′ ends of mammalian mitochondrial mRNAs. RNA. 2008; 14:862–871. [PubMed: 18367717]
22. Lancaster L, Noller HF. Involvement of 16S rRNA nucleotides G1338 and A1339 in discrimination of initiator tRNA. Mol Cell. 2005; 20:623–632. [PubMed: 16307925]
23. Montoya J, Ojala D, Attardi G. Distinctive features of the 5′-terminal sequences of the human mitochondrial mRNAs. Nature. 1981; 290:465–470. [PubMed: 7219535]
24. Bibb MJ, Van Etten RA, Wright CT, Walberg MW, Clayton DA. Sequence and gene organization of mouse mitochondrial DNA. Cell. 1981; 26:167–180. [PubMed: 7332926]
25. Crozier RH, Crozier YC. The mitochondrial genome of the honeybee Apis mellifera: complete sequence and genome organization. Genetics. 1993; 133:97–117. [PubMed: 8417993]
26. Cromsigt J, van Buuren B, Schleucher J, Wijmenga S. Resonance assignment and structure determination for RNA. Methods Enzymol. 2001; 338:371–399. [PubMed: 11460559]
27. Lill R, Robertson JM, Wintermeyer W. Affinities of tRNA binding sites of ribosomes from *Escherichia coli*. Biochemistry. 1986; 25:3245–3255. [PubMed: 3524675]
28. Laursen BS, Sørensen HP, Mortensen KK, Sperling-Petersen HU. Initiation of protein synthesis in bacteria. Microbiol Mol Biol Rev. 2005; 69:101–123. [PubMed: 15755955]

29. Takeuchi N, Kawakami M, Omori A, Ueda T, Spremulli LL, Watanabe K. Mammalian mitochondrial methionyl-tRNA transformylase from bovine liver. Purification, characterization, and gene structure. J Biol Chem. 1998; 273:15085–15090. [PubMed: 9614118]
30. Spencer AC, Heck A, Takeuchi N, Watanabe K, Spremulli LL. Characterization of the human mitochondrial methionyl-tRNA synthetase. Biochemistry. 2004; 43:9743–9754. [PubMed: 15274629]
31. Nakamura Y, Gojobori T, Ikemura T. Codon usage tabulated from international DNA sequence databases: status for the year 2000. Nucleic Acids Res. 2000; 28:292. [PubMed: 10592250]
32. Scheffler, IE. Mitochondria. John Wiley & Sons, Inc.; Hoboken, New Jersey: 2008.
33. Moore PB. Structural motifs in RNA. Annu Rev Biochem. 1999; 68:287–300. [PubMed: 10872451]
34. Auffinger P, Westhof E. An extended structural signature for the tRNA anticodon loop. RNA. 2001; 7:334–341. [PubMed: 11333014]
35. Ashraf SS, Ansari G, Guenther R, Sochacka E, Malkiewicz A, Agris PF. The uridine in “U-turn”: contributions to tRNA-ribosomal binding. RNA. 1999; 5:503–511. [PubMed: 10199567]
36. Murphy FV, Ramakrishnan V, Malkiewicz A, Agris PF. The role of modifications in codon discrimination by $tRNA^{Lys}_{UUU}$. Nat Struct Mol Biol. 2004; 11:1186–1191. [PubMed: 15558052]
37. Gustilo EM, Vendeix FAP, Agris PF. tRNA's modifications bring order to gene expression. Curr Opin Microb. 2008; 11:134–140.
38. Lescrinier E, Nauwelaerts K, Zanier K, Poesen K, Sattler M, Herdewijn P. The naturally occurring N^6-threonyl adenine in anticodon loop of *Schizosaccharomyces pombe* tRNAi causes formation of a unique U-turn motif. Nucleic Acids Res. 2006; 34:2878–2886. [PubMed: 16738127]
39. Agris PF. Bringing order to translation: Contributions of tRNA anticodon domain modifications. EMBO Reports. 2008; 9:629–635. [PubMed: 18552770]
40. Zacharias M, Sklenar H. Conformational analysis of single-base bulges in A-form DNA and RNA using a hierarchical approach and energetic evaluation with a continuum solvent model. J Mol Biol. 1999; 289:261–275. [PubMed: 10366504]
41. Schweisguth DC, Moore PB. On the conformation of the anticodon loops of initiator and elongator methionine tRNAs. J Mol Biol. 1997; 267:505–519. [PubMed: 9126834]
42. Ramesh V, RajBhandary UL. Importance of the anticodon sequence in the aminoacylation of tRNAs by methionyl-tRNA synthetase and by valyl-tRNA synthetase in an Archaebacterium. J Biol Chem. 2001; 276:3660–3665. [PubMed: 11058596]
43. Senger B, Fasiolo F. Yeast $tRNA^{Met}$ recognition by methionyl-tRNA synthetase requires determinants from the primary, secondary and tertiary structure: a review. Biochimie. 1996; 78:597–604. [PubMed: 8955903]
44. Pelka H, Schulman LH. Study of the interaction of *Escherichia coli* methionyl-tRNA synthetase with $tRNA_f^{Met}$ using chemical and enzymatic probes. Biochemistry. 1986; 25:4450–4456. [PubMed: 3092857]
45. Nakanishi K, Ogiso Y, Nakama T, Fukai S, Nureki O. Structural basis for anticodon recognition by methionyl-tRNA synthetase. Nat Struct Mol Biol. 2005; 12:931–932. [PubMed: 16155581]
46. (16) Kawai G, Yokogawa T, Nishikawa K, Ueda T, Hashizume T, McCloskey JA, Yokoyama S, Watanabe K. Conformational properties of a novel modified nucleoside, 5-formylcytidine, found at the first position of the anticodon of mitochondrial $tRNA^{Met}$. Nucleosides, Nucleotides and Nucleic acids. 1994; 13:1189–1199.
47. Agris PF, Vendeix FAP, Graham WD. tRNA's wobble decoding of the genome: 40 years of modification. J Mol Biol. 2006; 366:1–13. [PubMed: 17187822]
48. Weixlbaumer A, Murphy F IV, Vendeix FAP, Dziergowska A, Malkiewicz A, Agris PF, Ramakrishnan V. Mechanism for expanding the decoding capacity of transfer RNAs by modification of uridines. Nature Struct Mol Biol. 2007; 14:498–502. [PubMed: 17496902]
49. Vendeix FAP, Graham WD, Dziergowska A, Gustilo E, Sproat B, Malkiewicz A, Agris PF. Anticodon domain modifications contribute order to tRNA for ribosome-mediated codon binding. Biochemistry. 2008; 47:6117–6129. [PubMed: 18473483]

50. Barraud P, Schmitt E, Mechulam Y, Dardel F, Tisne C. A unique conformation of the anticodon stem-loop is associated with the capacity of tRNAfMet to initiate protein synthesis. Nucleic Acids Res. 2008; 36:4894–4901. [PubMed: 18653533]
51. Basavappa R, Sigler PB. The 3 A crystal structure of yeast initiator tRNA: functional implications in initiator/elongator discrimination. EMBO J. 1991; 10:3105–3111. [PubMed: 1915284]
52. Schevitz RW, Podjarny AD, Krishnamachari N, Hughes JJ, Sigler PB, Sussman JL. Crystal structure of a eukaryotic initiator tRNA. Nature. 1979; 278:188–190. [PubMed: 368656]
53. Woo NH, Roe BA, Rich A. Three-dimensional structure of Escherichia coli initiator $tRNA^{fMet}$. Nature. 1980; 286:346–351. [PubMed: 6157105]
54. Nakanishi K, Ogiso Y, Nakama T, Fukai S, Nureki O. Structural basis for anticodon recognition by methionyl-tRNA synthetase. Nat Struct Mol Biol. 2005; 12:931–932. [PubMed: 16155581]
55. Perbandt M, Barciszewska MZ, Betzel C, Erdmann VA, Barciszewski J. A critical role of water in the specific cleavage of the anticodon loop of some eukaryotic methionine initiator tRNAs. Mol Biol Rep. 2003; 30:27–31. [PubMed: 12688532]
56. Dix DB, Wittenberg WL, Uhlenbeck OC, Thompson RC. Effect of replacing uridine 33 in yeast $tRNA^{Phe}$ on the reaction with ribosomes. J Biol Chem. 1986; 261:10112–10118. [PubMed: 2426258]
57. Wrede P, Woo NH, Rich A. Initiator tRNAs have a unique anticodon loop conformation. Proc Natl Acad Sci USA. 1979; 76:3289–3293. [PubMed: 386336]
58. Ramakrishnan V. Ribosome Structure and the Mechanism of Translation. Cell. 2002; 108:557–572. [PubMed: 11909526]
59. Selmer M, Dunham CM, Murphy FV, Weixlbaumer A, Petry S, Kelley AC, Weir JR, Ramakrishnan V. Structure of the 70S ribosome complexed with mRNA and tRNA. Science. 2006; 313:1935–1942. [PubMed: 16959973]
60. Roy A, Panigrahi S, Bhattacharyya M, Bhattacharyya D. Structure, stability, and dynamics of canonical and noncanonical base pairs: Quantum chemical studies. J Phys Chem B. 2008; 112:3786–3796. [PubMed: 18318519]
61. Vendeix FAP, Munoz A, Agris PF. Free energy calculation of modified base-pair formation in explicit solvent: A predictive model. RNA. 2009; 15:2278–2287. [PubMed: 19861423]
62. Cai Z, Tinoco I Jr. Solution structure of loop A from the hairpin ribozyme from tobacco ringspot virus satellite. Biochemistry. 1996; 35:6026–6036. [PubMed: 8634244]
63. Scaringe SA. Advanced 5′-silyl-2′-orthoester approach to RNA oligonucleotide synthesis. Methods Enzymol. 2000; 317:3–18. [PubMed: 10829269]
64. Wüthrich, K. NMR of Proteins and Nucleic Acids. John Wiley & Sons, Inc.; Hoboken, New Jersey: 1986.
65. Delaglio F, Grzesiek S, Vuister GW, Zhu G, Pfeifer J, Bax A. NMRPipe: a multidimensional spectral processing system based on UNIX pipes. J Biomol NMR. 1995; 6:277–293. [PubMed: 8520220]
66. Goddard, TD.; Kneller, D. G SPARKY 3.113. University of California; San Francisco: 2006. http://www.cgl.ucsf.edu/home/sparky/
67. Brünger AT, Adams PD, Clore GM, DeLano WL, Gros P, Grosse-Kunstleve RW, Jiang JS, Kuszewski J, Nilges M, Pannu NS, Read RJ, Rice LM, Simonson T, Warren GL. Crystallography & NMR system: A new software suite for macromolecular structure determination. Acta Crystallogr D Biol Crystallogr. 1998; 54(Pt 5):905–921. [PubMed: 9757107]
68. Brünger AT. Version 1.2 of the Crystallography and NMR system. Nat Protoc. 2007; 2:2728–2733. [PubMed: 18007608]
69. Stein EG, Rice LM, Brünger AT. Torsion-angle molecular dynamics as a new efficient tool for NMR structure calculation. J Magn Reson. 1997; 124:154–164. [PubMed: 9424305]
70. Lu XJ, Olson WK. 3DNA: a versatile, integrated software system for the analysis, rebuilding and visualization of three-dimensional nucleic-acid structures. Nat Protoc. 2008; 3:1213–1227. [PubMed: 18600227]
71. Koradi R, Billeter M, Wüthrich K. MOLMOL: a program for display and analysis of macromolecular structures. J Mol Graph. 1996; 14:51–5. 29–32. [PubMed: 8744573]

72. Shapkina T, Lappi S, Franzen S, Wollenzien P. Efficiency and pattern of UV pulse laser-induced RNA-RNA cross-linking in the ribosome. Nucleic Acids Res. 2004; 32:1518–1526. [PubMed: 14999094]

73. Brooke BE, Haque ME, Spremulli LL. The effect of spermine on the initiation of mitochondrial protein synthesis. Biochem Biophys Res Commn. 2010; 391:942–946.

74. Grasso DG, Christian BE, Spencer A, Spremulli LL. Overexpression and purification of mammalian mitochondrial translational initiation factor 2 and initiation factor 3. Methods Enzymol. 2007; 430:59–78. [PubMed: 17913635]

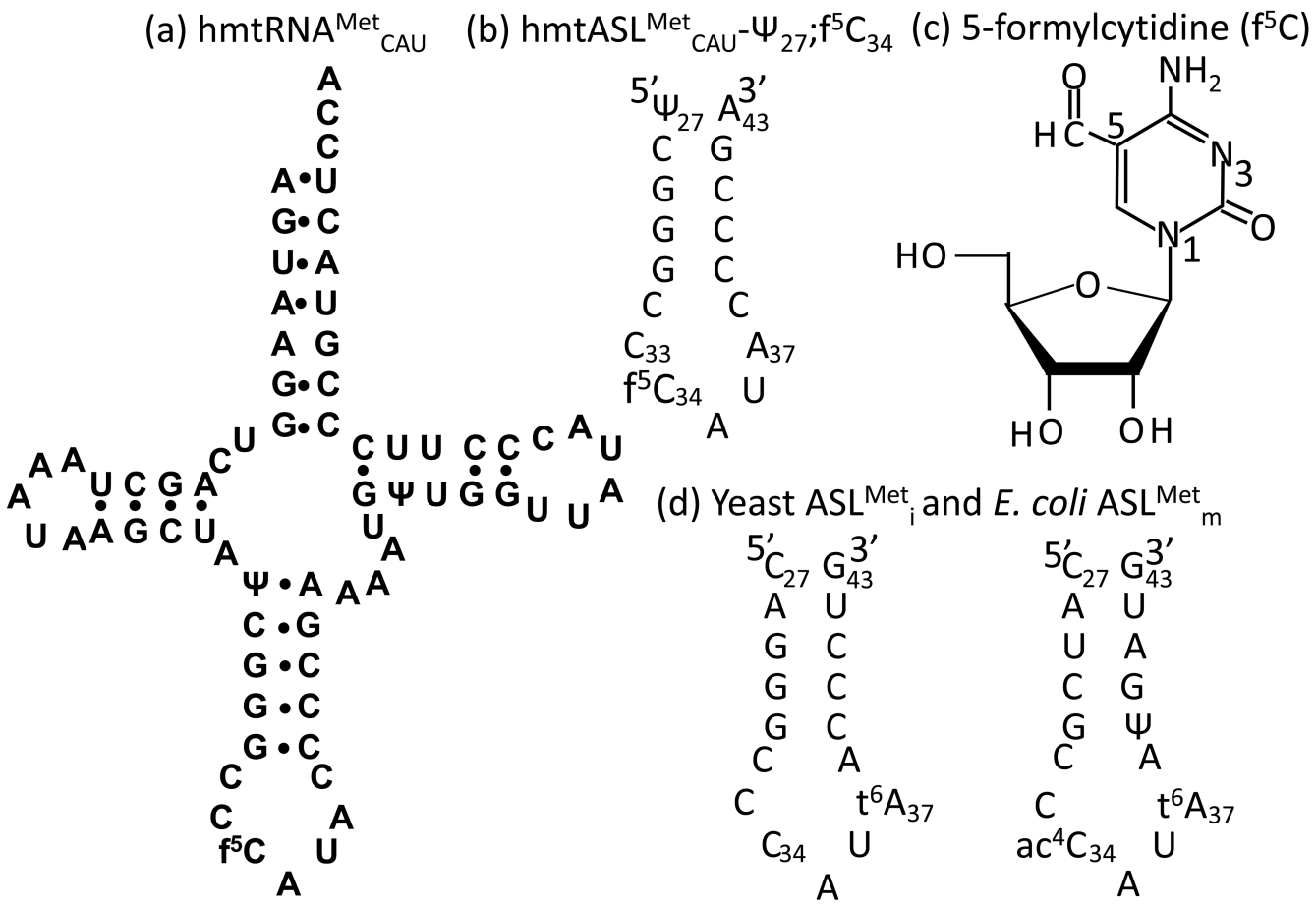

Figure 1.

Primary sequence and secondary structure of the human mtRNA$^{Met}_{CAU}$ and its anticodon stem and loop domain (hmtASL$^{Met}_{CAU}$-Ψ$_{27}$;f^{5}C$_{34}$). Primary sequence and secondary structure of the human (a) mtRNA$^{Met}_{CAU}$ and the (b) hmtASL$^{Met}_{CAU}$-Ψ$_{27}$;f^{5}C$_{34}$. (c) Chemical structure of the 5-formylcytidine modification, f^{5}C$_{34}$. Numbering of the nucleobase atoms is shown. (d) Nucleoside sequence and secondary structure of the anticodon stem and loop domains of the yeast tRNA$^{Met}_{i}$ (left) and *E.coli* tRNA$^{Met}_{m}$ (right).

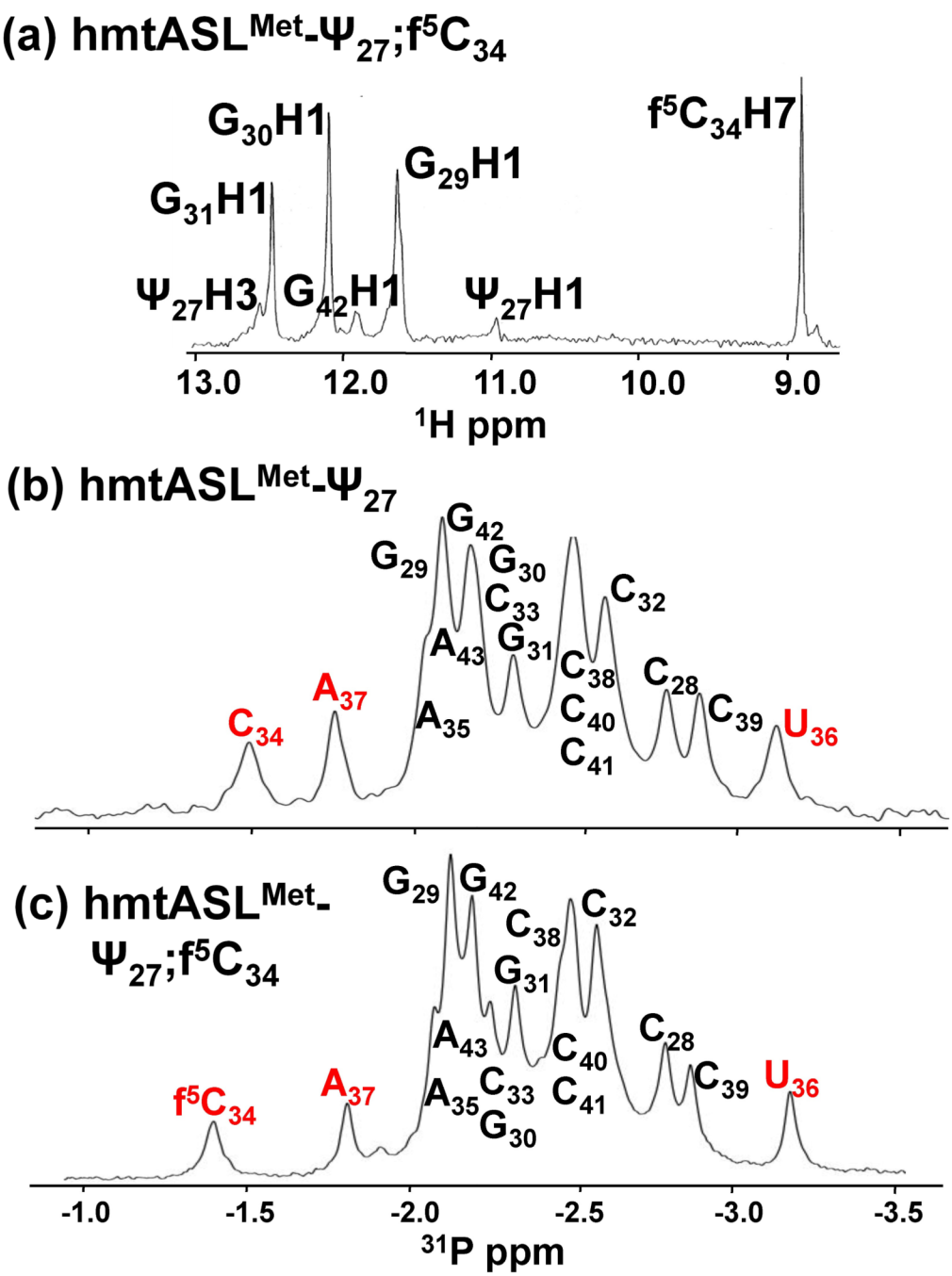

Figure 2.

^{1}H and ^{31}P NMR spectra (1D) of the hmtASL$^{Met}_{CAU}$. (a) ^{1}H NMR spectrum of the hmtASL$^{Met}_{CAU}$-Ψ_{27};f^5C_{34}. The H_2O-exchangeable proton resonances, as well as the formyl-proton (H7) resonance of f^5C_{34} are shown. (b) ^{31}P-NMR spectra (1D) of the hmtASL$^{Met}_{CAU}$-Ψ_{27} (top) and the hmtASL$^{Met}_{CAU}$-Ψ_{27};f^5C_{34} (bottom). The ^{31}P resonances for f^5C_{34}, C_{34}, A_{37} and U_{36} are denoted in red.

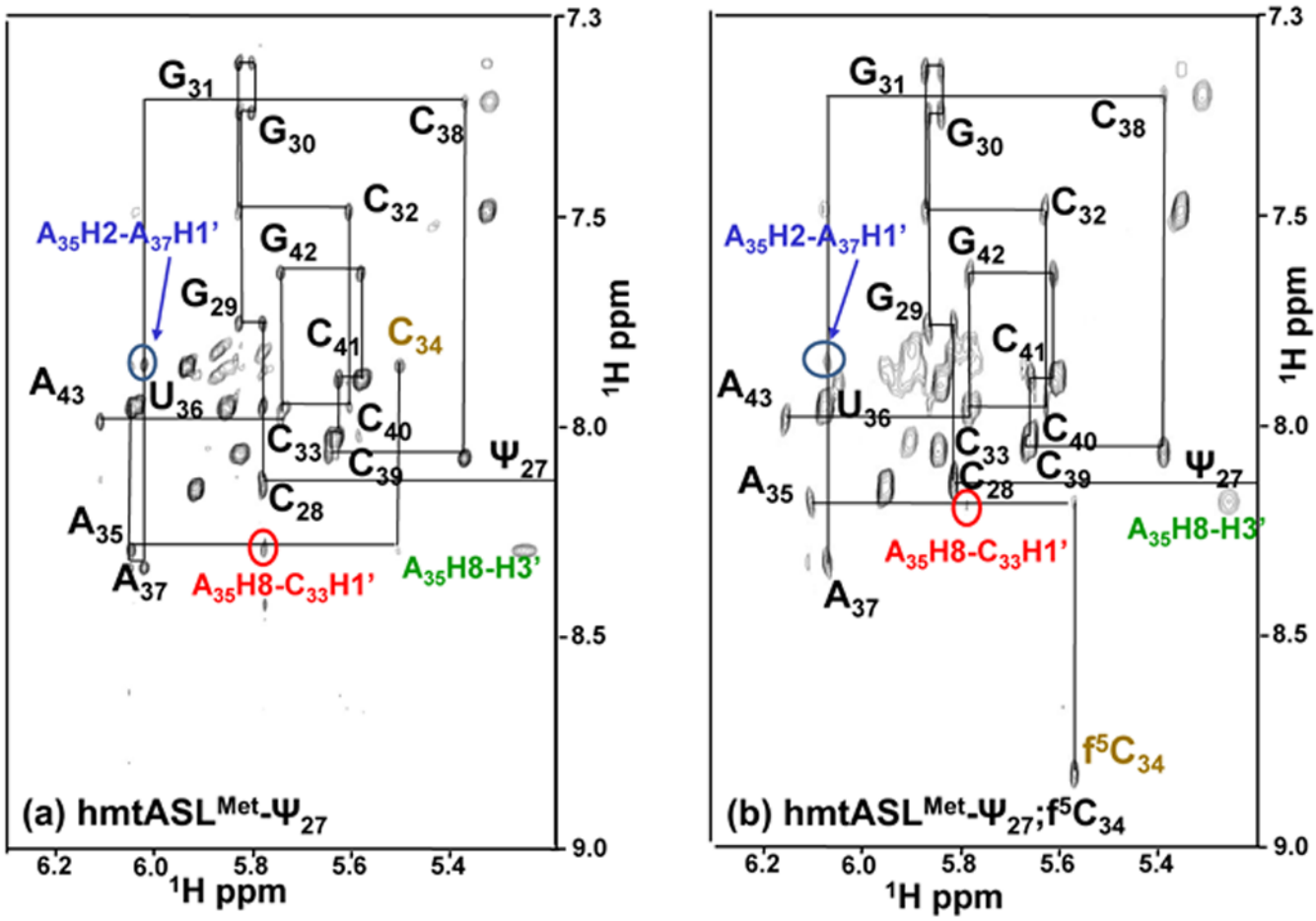

Figure 3.

The hmtASL$^{Met}_{CAU}$ NOSEY spectra. NOESY spectra of hmtASL$^{Met}_{CAU}$-Ψ_{27};f^5C_{34} (a) and hmtASL$^{Met}_{CAU}$-Ψ_{27} (b). NOSEY spectra of the hmtASL$^{Met}_{CAU}$ in D_2O were recorded at 25° C with a mixing time of 400 ms. The H1′ and H5 to aromatic portion of the spectra are shown. The sequential H1′-aromatic connectivities are indicated, as well as the unusual NOEs connectivities between $A_{35}H2 – A_{37}H1'$ (blue) and $A_{35}H8 – C_{33}H1'$ (red).

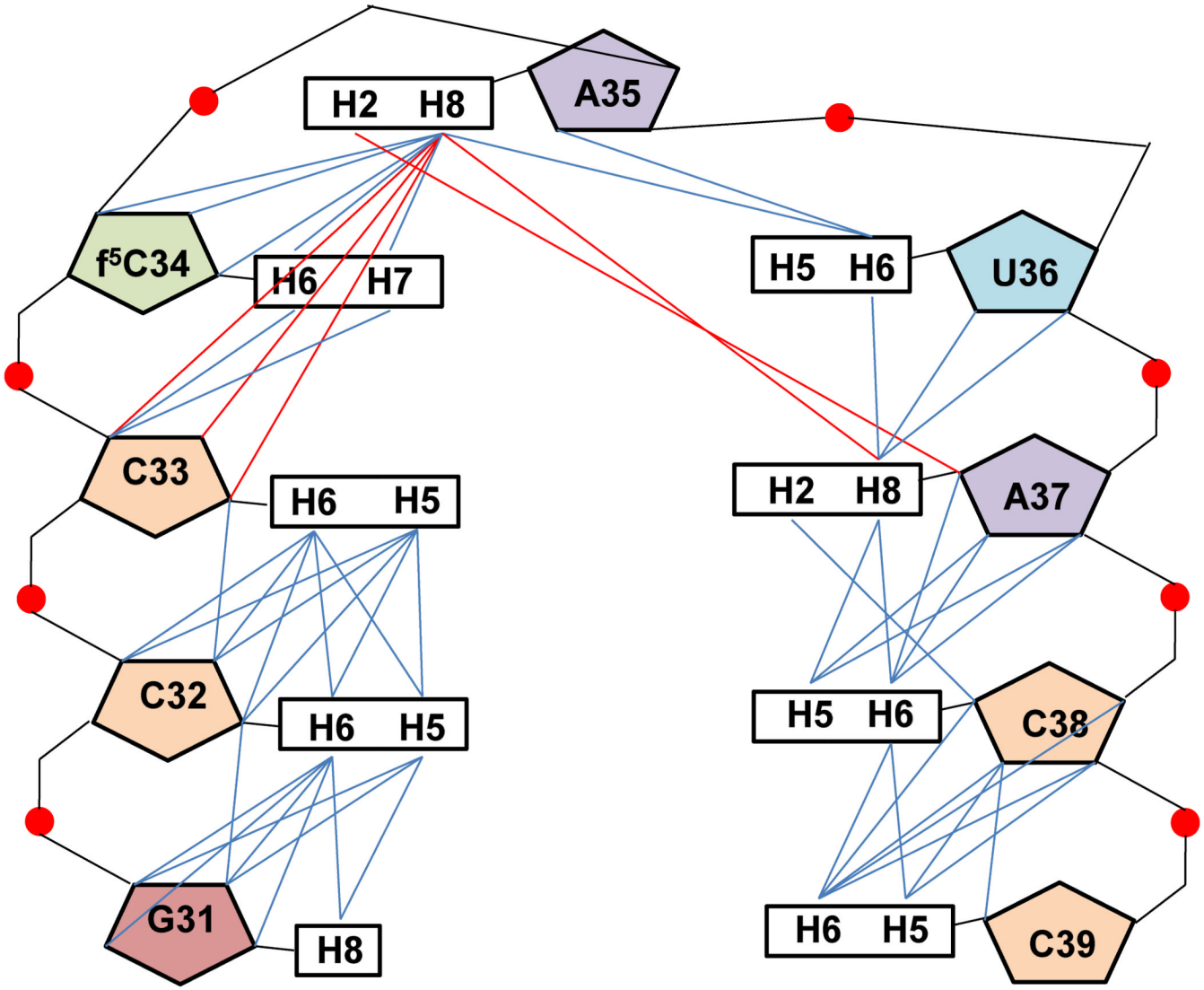

Figure 4.

Compilation of inter-nucleoside NOE connectivities. The inter-nucleoside NOEs observed in the loop residues 31 to 39 of the hmtASL$^{Met}_{CAU}$-Ψ_{27};f^5C_{34} were both sequential and non-sequential. The sequential (i to i+1) inter-nucleosides NOEs are shown in blue and the nonsequential NOEs are shown in red. The hmtASL$^{Met}_{CAU}$-Ψ_{27} exhibited comparable NOEs.

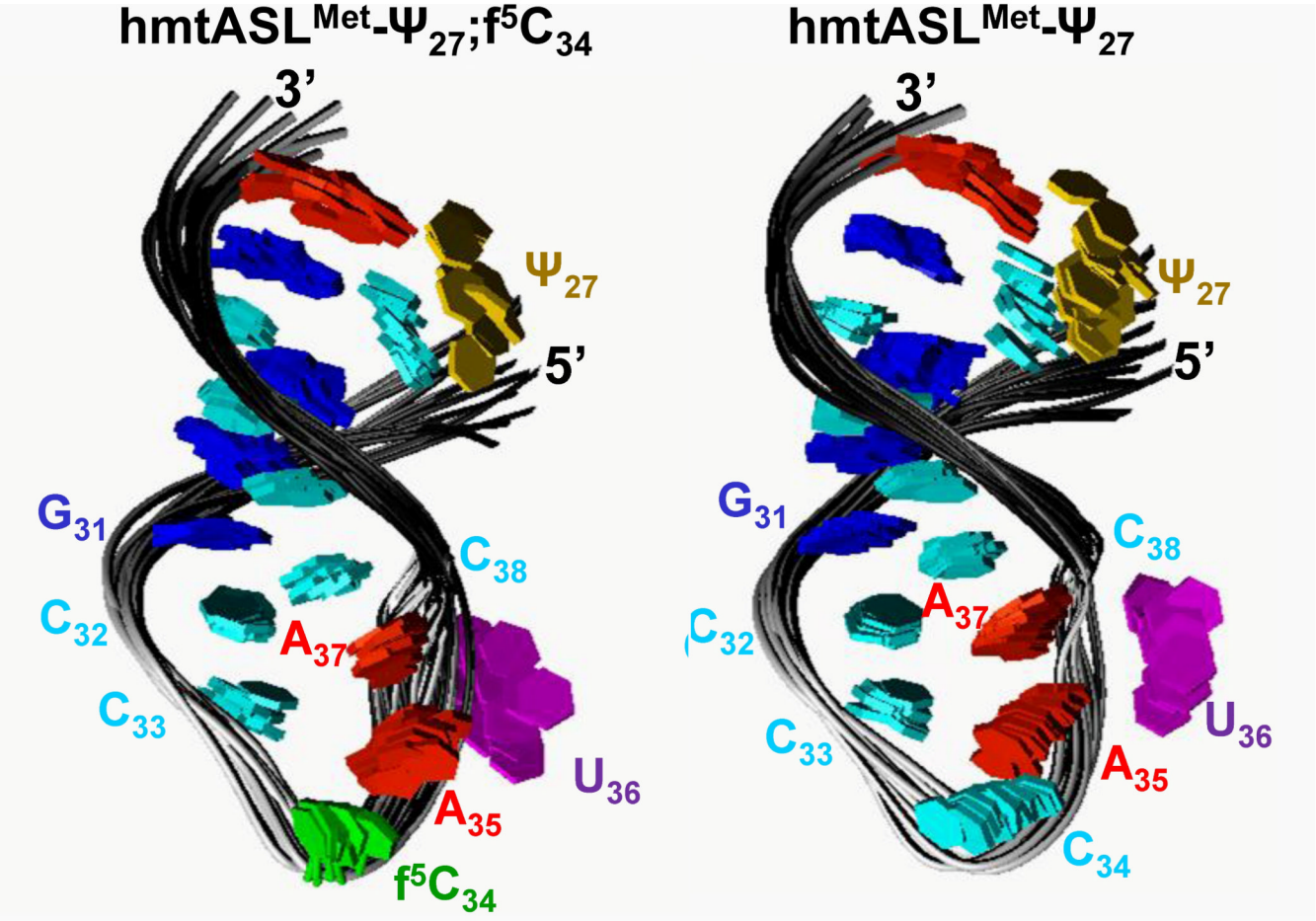

Figure 5.
Structures of the hmtASL$^{Met}_{CAU}$-Ψ$_{27}$;f^{5}C$_{34}$ and hmtASL$^{Met}_{CAU}$-Ψ$_{27}$. The ten lowest energy structures for the hmtASL$^{Met}_{CAU}$-Ψ$_{27}$;f^{5}C$_{34}$ (a) and those for the hmtASL$^{Met}_{CAU}$-Ψ$_{27}$ (b) are superimposed. To illustrate differences in the degree to which the bases of a family of structures converge, the ribose and phosphodiester bond details are not shown.

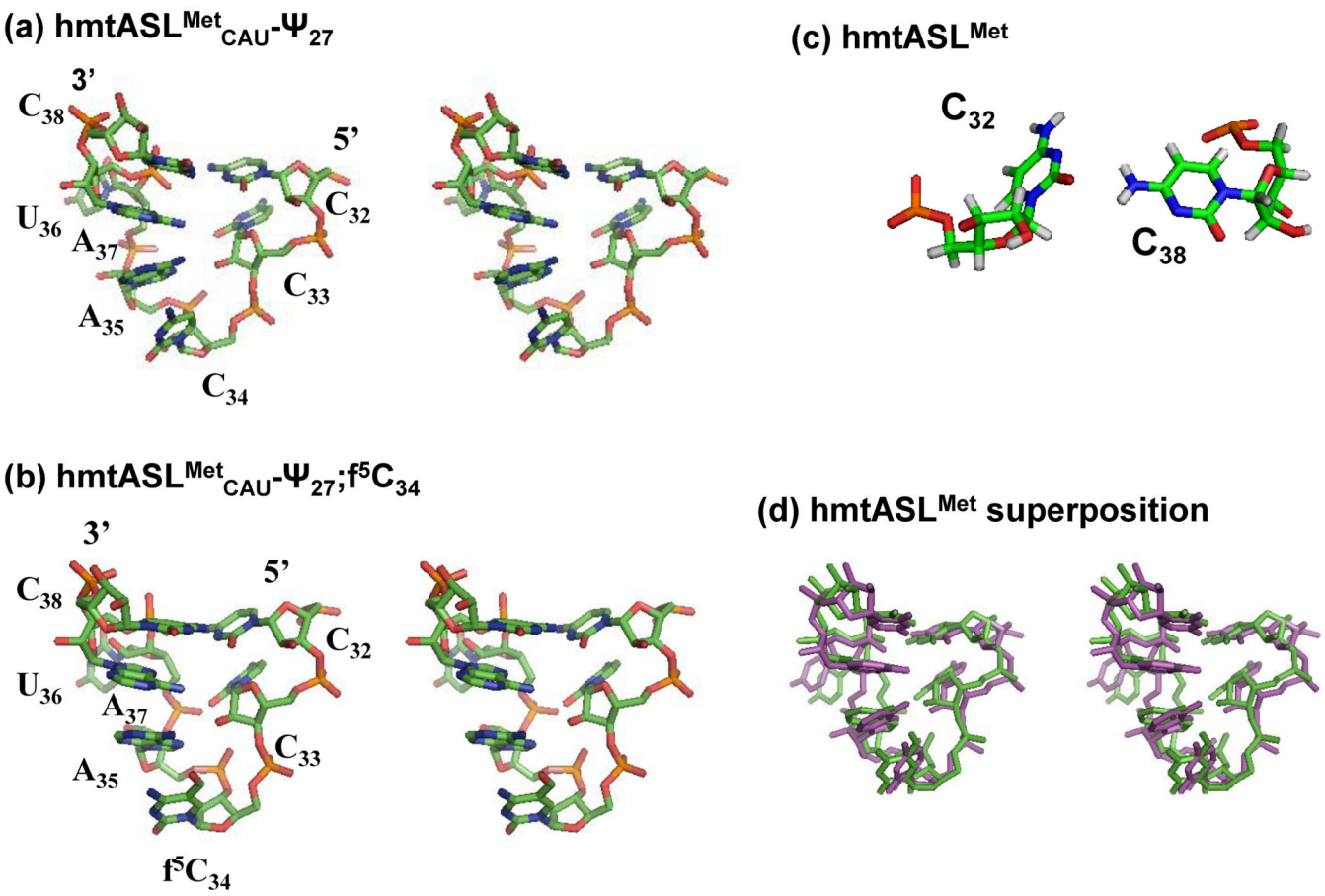

Figure 6.

Conformational differences and similarities in the anticodon loops of the f^{5}C$_{34}$-modified and unmodified hmtASL$^{Met}_{CAU}$-Ψ$_{27}$. Stereo view of the average structures of the anticodon loops (residues C$_{32}$ to A$_{38}$) for (a) hmtASL$^{Met}_{CAU}$-Ψ$_{27}$ and (b) hmtASL$^{Met}_{CAU}$-Ψ$_{27}$;f^{5}C$_{34}$. (c) The anticodon loops contain a C$_{32}$●C$_{38}$ intra-loop base pair in both the hmtASL$^{Met}_{CAU}$-Ψ$_{27}$;f^{5}C$_{34}$ and the hmtASL$^{Met}_{CAU}$-Ψ$_{27}$. (d) Stereo view of the two average structures superimposed (green, hmtASL^{Met}-Ψ$_{27}$;f^{5}C$_{34}$; and purple, the hmtASL$^{Met}_{CAU}$-Ψ$_{27}$).

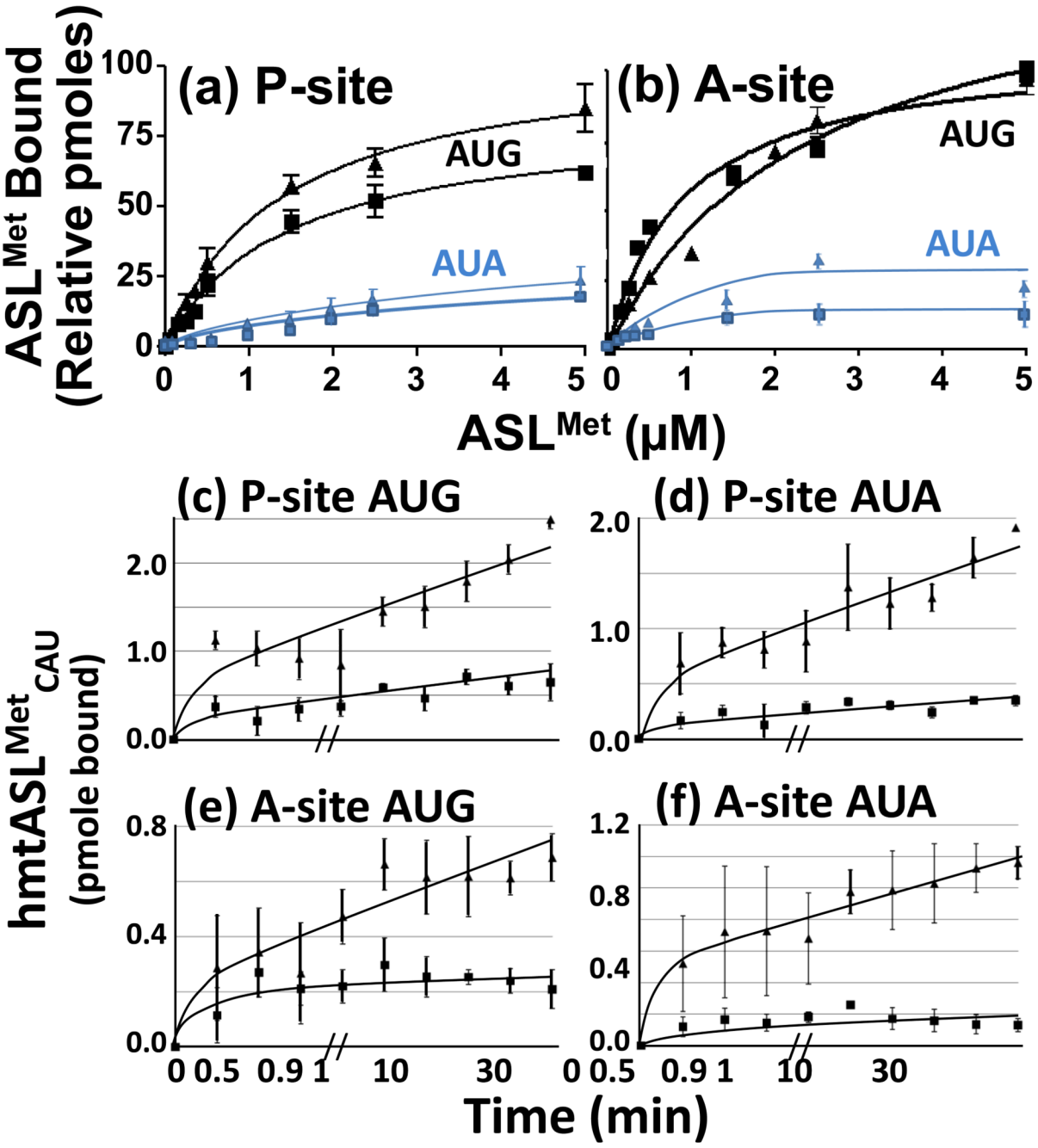

Figure 7.

AUG and AUA codon binding properties of the hmtASL$^{Met}_{CAU}$-Ψ_{27};f^5C_{34} and hmtASL$^{Met}_{CAU}$-Ψ_{27} in the P- and A-sites of the ribosome. (a) AUG and AUA codon binding of the hmtASL$^{Met}_{CAU}$-Ψ_{27};f^5C_{34} and hmtASL$^{Met}_{CAU}$-Ψ_{27} in the P-site of the ribosome. The *E. coli* 70S ribosome (5 pmoles), programmed with AUG in the P-site, was titrated with hmtASL$^{Met}_{CAU}$-Ψ_{27};f^5C_{34} (▲) and with hmtASL$^{Met}_{CAU}$-Ψ_{27} (■), or programmed with AUA and titrated with hmtASL$^{Met}_{CAU}$-Ψ_{27};f^5C_{34} (▲) and with hmtASL$^{Met}_{CAU}$-Ψ_{27} (■). The maximum hmtASL$^{Met}_{CUA}$ bound was between 3-4 pmoles. (b) AUG and AUA codon binding properties of the hmtASL$^{Met}_{CAU}$-Ψ_{27};f^5C_{34} and hmtASL$^{Met}_{CAU}$-Ψ_{27} in the A-site of the ribosome. The *E. coli* 70S ribosome (5 pmoles),

programmed with AUG in the A-site, was titrated with hmtASL$^{Met}_{CAU}$-Ψ$_{27}$;f^{5}C$_{34}$ (▲) and with hmtASL$^{Met}_{CAU}$-Ψ$_{27}$ (■), or programmed with AUA and titrated with hmtASL$^{Met}_{CAU}$-Ψ$_{27}$;f^{5}C$_{34}$ (▲) and with hmtASL$^{Met}_{CAU}$-Ψ$_{27}$ (■). The maximum hmtASL$^{Met}_{CUA}$ bound was between 0.5-1.0 pmoles. In contrast to equilibrium binding studies, the time-dependent binding of the hmtASL$^{Met}_{CAU}$-Ψ$_{27}$;f^{5}C$_{34}$ (▲) and hmtASL$^{Met}_{CAU}$-Ψ$_{27}$ (■) to AUG and AUA were conducted at the single concentration of ASL (0.5 μM), far too low to saturate the ribosomes. The hmtASL$^{Met}_{CAU}$-Ψ$_{27}$;f^{5}*C*$_{34}$ and hmtASL$^{Met}_{CAU}$-Ψ$_{27}$ were bound to (c) AUG in the P-site of *E. coli* 70S ribosome, and to (d) AUA in the P-site). The hmtASL$^{Met}_{CAU}$-Ψ$_{27}$;f^{5}C$_{34}$ and hmtASL$^{Met}_{CAU}$-Ψ$_{27}$ were bound to (e) AUG in the A-site of *E. coli* 70S ribosome, and to (f) AUA in the A-site.

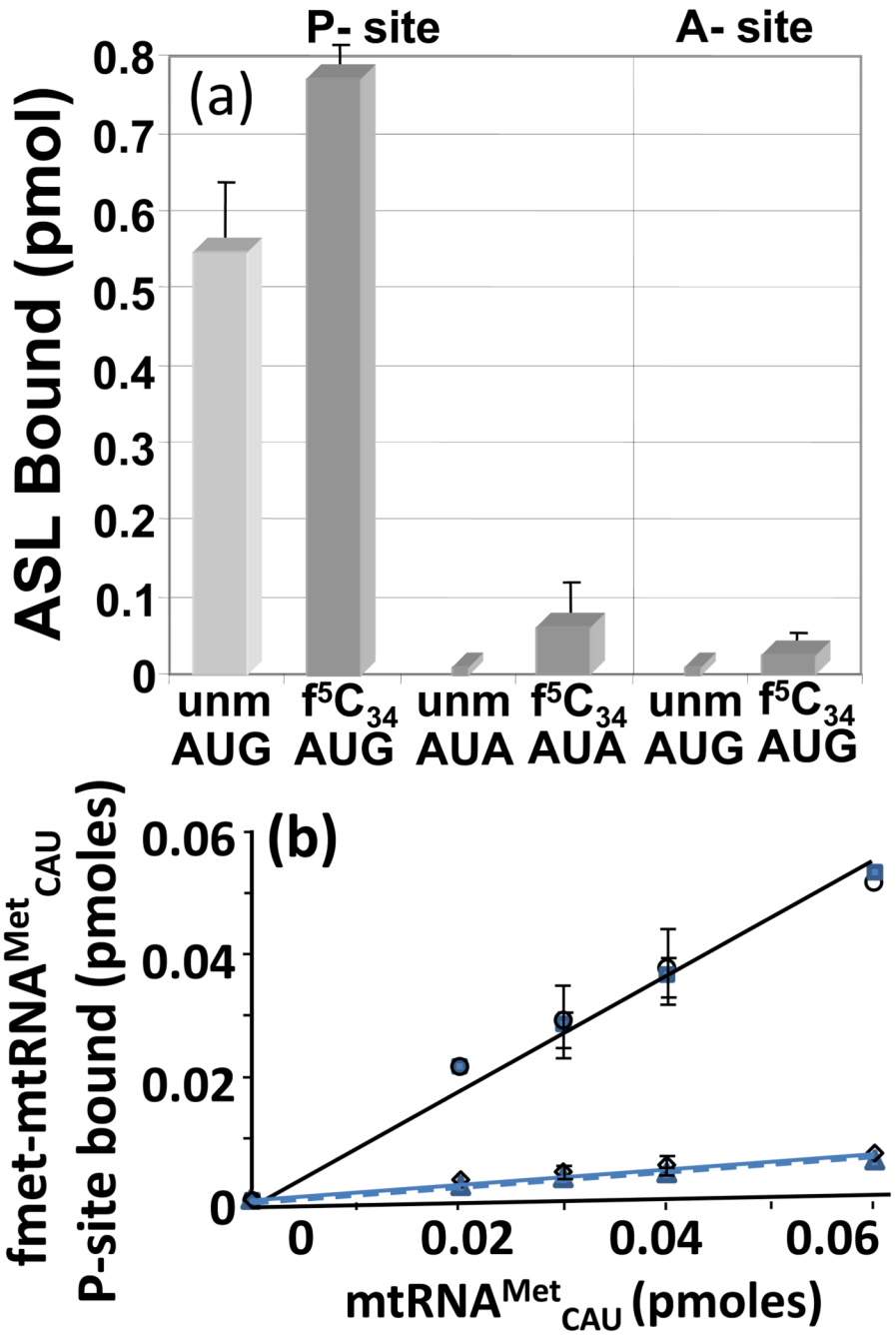

Figure 8.

Codon binding by hmtASL$^{Met}_{CAU}$, the native hmtRNA$^{Met}_{CAU}$ and the unmodified transcript on the bovine mitochondrial ribosome. (a) AUG and AUA codon binding by the hmtASL$^{Met}_{CAU}$-Ψ_{27};f^5C_{34} (f^5C_{34}) and hmtASL$^{Met}_{CAU}$-Ψ_{27} (unm) on the 55S bovine mitochondrial ribosome. The modification f^5C_{34} enhanced P-site binding of the AUG and AUA codons, and A-site binding to the AUG codon. However, A-site binding of the AUA codon by either ASL was not detectable. The binding (pmoles) of hmtASL$^{Met}_{CAU}$-Ψ_{27};f^5C_{34} and hmtASL$^{Met}_{CAU}$-Ψ_{27} are shown under conditions in which the ASLs are saturating. **(b)** The IF2-facilitated binding of bovine mtRNA$^{Met}_{CAU}$ and its transcript to AUG and AUA in the P-site of the bovine mitochondrial ribosome. The bovine

mitochondrial ribosome programmed with AUG was titrated with either $mtRNA^{Met}_{CAU}$ (○) or its transcript (■). Also, the AUA-programmed ribosome was titrated with either $mtRNA^{Met}_{CAU}$ (◊) or its transcript (▲).

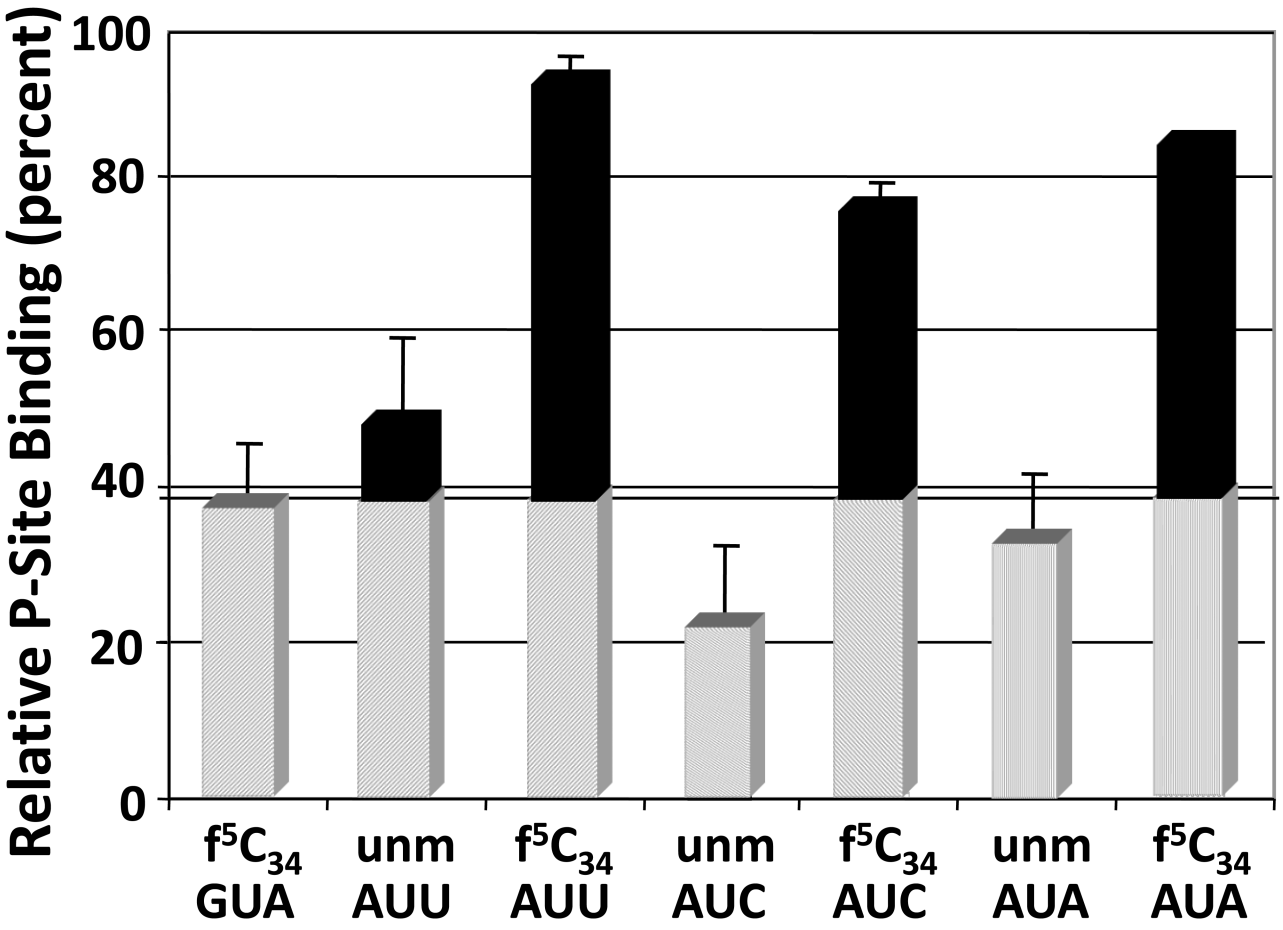

Figure 9.

The f^5C_{34}-modified hmtASL$^{Met}_{CAU}$-Ψ_{27} binds the near-cognate codons AUU and AUC. The modification f^5C_{34} enabled hmtASL$^{Met}_{CAU}$-Ψ_{27};f^5C_{34} to bind the near-cognate codons AUU and AUC, as well as AUA, in the P-site of the *E. coli* ribosome. The relative binding of non-cognate codons by hmtASL$^{Met}_{CAU}$-Ψ_{27};f^5C_{34} (f^5C_{34}) and hmtASL$^{Met}_{CAU}$-Ψ_{27} (unm) are shown under conditions in which the ribosomes are saturated with ASLs, and the results internally normalized (percent). The binding of the valine codon GUA by hmtASL$^{Met}_{CAU}$-Ψ_{27};f^5C_{34} (f^5C_{34}) is an indication of the degree of non-specific binding in the assay.

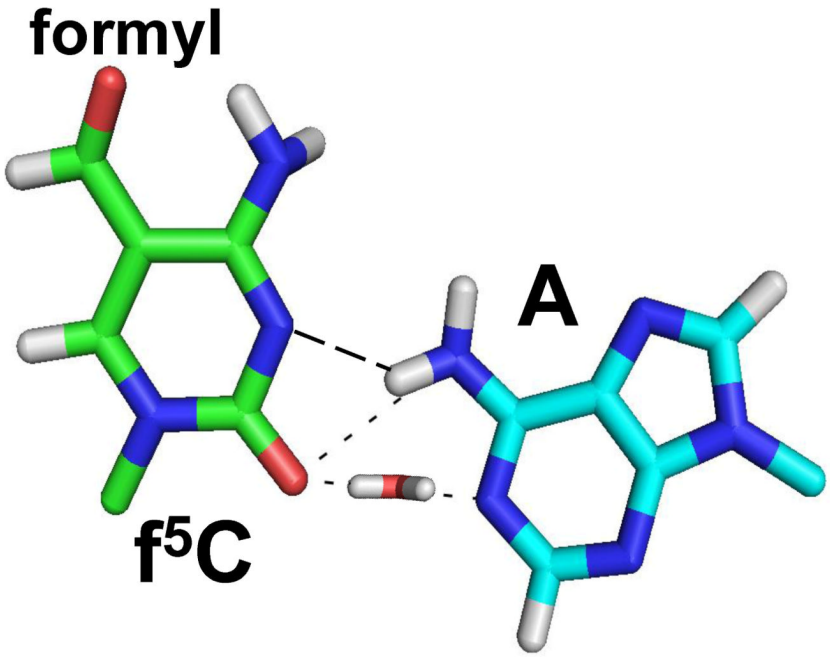

Figure 10.

Molecular dynamics simulation of the f^5C_{34}●A base pair. The f^5C_{34}●A base pair must occur on the mitochondrial ribosome when $hmtRNA^{Met}_{CAU}$ reads the AUA codon in either the A-or P-sites. The base pairing of the 5′-monophosphate of f^5C_{34} with that of A under aqueous and neutral conditions was simulated with molecular dynamics,[61] and the lowest energy structure is presented here. The resulting model indicated a possible bridging H_2O molecule that stabilizes the interaction.

Table 1

Structural statistics for hmtASL $^{Met}_{CAU}$-Ψ$_{27}$;f^{5}C$_{34}$ and hmtASL $^{Met}_{CAU}$-Ψ$_{27}$

	hmtASL $^{Met}_{CAU}$-Ψ$_{27}$;f^{5}C$_{34}$	hmtASL $^{Met}_{CAU}$-Ψ$_{27}$
Number of experimental restraints		
Distance restraints	266	275
Intranucleotides	157	161
Internucleotides	109	114
Exchangeable	13	13
Restraints by residue	15.6	16.1
Hydrogen bonding distances restraints	24	24
Dihedral restraints	82	82
Negative NOEs	26	25
Heavy atoms RMSD from mean structure (Å)		
All residues (Y_{27} - A_{43})	1.51 ± 0.58	1.71 ± 0.58
Loop residues (C_{32} – C_{38})	0.51 ± 0.17	0.38 ± 0.20

Table 2

Dissociation constants (K_d) of Unmodified and f^5C_{34}-Modified $hmtASL^{Met}_{CAU}$-Ψ_{27} for the Mitochondrial methionine Codons at the *E. coli* Ribosomal P or A-sites

Dissociation Constants (K_d, μM)				
$hmtASL^{Met}_{CAU}$-Ψ_{27}	P-site		A-site	
	AUG	*AUA*	*AUG*	*AUA*
unmodified	1.4 ± 0.29	11.0 ± 4.7	0.9 ± 0.1	4.5 ± 2.1
f^5C_{34}	1.3 ± 0.22	7.9 ± 5.5	2.4 ± 0.4	1.6 ± 0.4